TOPOLOGY DESIGN OF VLASOV BEAM SECTIONS

A THESIS SUBMITTED TO
THE GRADUATE SCHOOL OF NATURAL AND APPLIED SCIENCES
OF
MIDDLE EAST TECHNICAL UNIVERSITY

BY

FATİH ÇETİN

IN PARTIAL FULFILLMENT OF THE REQUIREMENTS
FOR
THE DEGREE OF MASTER OF SCIENCE
IN
MECHANICAL ENGINEERING

SEPTEMBER 2019

Approval of the thesis:

TOPOLOGY DESIGN OF VLASOV BEAM SECTIONS

submitted by **FATİH ÇETİN** in partial fulfillment of the requirements for the degree of **Master of Science in Mechanical Engineering Department, Middle East Technical University** by,

Prof. Dr. Halil Kalıpçılar
Dean, Graduate School of **Natural and Applied Sciences**   _____

Prof. Dr. M.A. Sahir Arıkan
Head of Department, **Mechanical Engineering**   _____

Prof. Dr. Suha Oral
Supervisor, **Mechanical Engineering, METU**   _____

Examining Committee Members:

Prof. Dr. Haluk Darendeliler
Mechanical Engineering, METU   _____

Prof. Dr. Suha Oral
Mechanical Engineering, METU   _____

Prof. Dr. Serkan Dağ
Mechanical Engineering, METU   _____

Prof. Dr. Can Çoğun
Mechanical Engineering, Çankaya University   _____

Assoc. Prof. Dr. Uğur Polat
Civil Engineering, METU   _____

Date: 06.09.2019

I hereby declare that all information in this document has been obtained and presented in accordance with academic rules and ethical conduct. I also declare that, as required by these rules and conduct, I have fully cited and referenced all material and results that are not original to this work.

Name, Surname: Fatih Çetin

Signature:

ABSTRACT

TOPOLOGY DESIGN OF VLASOV BEAM SECTIONS

Çetin, Fatih
Master of Science, Mechanical Engineering
Supervisor: Prof. Dr. Suha Oral

September 2019, 80 pages

The optimal cross-section of beams plays an important role in load-carrying members. The section of a beam should be designed such that the structure carries higher loads with less weight. Some structures which are subjected to static combined loading require a continuous cross-section along their axial direction due to manufacturing reasons. In classical structural topology optimization methods, it is aimed to optimize the whole beam. However, these methods are impractical when optimize the whole beam as they generate beams with non-uniform topologies and varying cross-sections along the axial direction. On the other hand, most of the earlier studies address only the bending and torsional rigidity optimization of cross-sections, regardless of the loading on the beam in question. In this thesis, the topology optimization of Vlasov beam sections is studied according to Vlosov beam theory. For the purpose of this study an optimization method hereby known as the Evolutionary Growth Algorithm (EGA) was generated and through this algorithm it is proposed that the optimum cross-section can be found in accordance with the strength to area ratio. The optimization methodology generated in this thesis uses element Von Mises stress as a material addition and removal criterion and also takes symmetrical design constraints into account. Indeed, material addition and/or removal are decided according to the stress level of each element and the symmetry constraints of the cross-section. The cross section domain has to be coherent throughout its evolution, i.e. there should be no

disconnection between the elements. Therefore, a special algorithm is included in the Evolutionary Growth Algorithm (EGA) to check the connectivity of the active elements in the cross-section during element removal. At the end of the optimization process, it is aimed to have determined the optimum cross-section limit at which point the area will be minimized for the maximum Von Misses stress applied to the section. Both finite element analyses and optimization algorithm were coded in MATLAB and run consecutively to achieve the goal of this study.

ÖZ

VLASOV KİRİŞLERİNİN TOPOLOJİ TASARIMI

Çetin, Fatih
Yüksek Lisans, Makina Mühendisliği
Tez Danışmanı: Prof. Dr. Suha Oral

Eylül 2019, 80 sayfa

Optimum kiriş kesiti yük taşıma elemanlarında önemli rol oynar. Kiriş kesit alanı elemanları daha az ağırlıkla daha yüksek yükleri taşıyabilcek şekilde tasarlanabilmektedir. Çoklu durağan yüklemeye maruz kalan yapılar üretimden kaynaklanan sebeplerden dolayı eksenel yönleri boyunca sabit kesitler gerektirmektedir. Konvensiyonel optimizasyon metotlar yapının bir bütün olarak optimize edilmesi amaçlar.Ancak bu yaklaşımlar eksenel doğrultuda düzgün olmayan ve kesit alanları eksenel yönleri boyunca değişen kirişler üretir. Öte yandan daha önce yapılan çalışmalarda çoğu kiriş üzerindeki yükten bağımsız olarak kesitin sadece bükülme veya çarpılma ile ilişkisi incelenmiştir. Bu tez çalışmasından Vlasov Kirişi Optimizayonu yapılmıştır.Evrimsel Büyüme Algoritması olarak adlandırılan (EBA) optimizasyon yöntemi dayanım alan oranına göre en uygun kesiti elde etmek için geliştirilmiştir. Bu tezde geliştrilen optimizaston metodu simetrik tasarım ve Von Mises gerilimlerim kısıtlarını hesaba katarak oluşturulmuştur. Optimizasyon algoritmasında eleman çıkarma işlemi sırasında tüm kesit alanının bütünlüğünü koruduğu kontrol edilir. Sonlu eleman analizleri ve optimizasyon yöntemi MATLAB ortamında çalışmanın amacına ulaşmak için ardı ardına koşturulmaktadır.

Anahtar Kelimeler: Katı Cisimler Mekaniği, Vlasov Kirişleri, Kesit Alanı,Yapısal Optimizasyon, Sonlu Elemanlar Analizi

To: My Wife Dilara, My Family, My Colleagues

ACKNOWLEDGEMENTS

TABLE OF CONTENTS

LIST OF TABLES

TABLES

LIST OF FIGURES

FIGURES

LIST OF ABBREVIATIONS

BESO   Bi-directional evolutionary structural optimization

ESO   Evolutionary structural optimization

FEA   Finite element analysis

GA   Genetic Algorithm

IR   Inclusion Rate

OC   Optimality criterion

RC   Reduction Coefficient

symy   Symmetry about y axis

symz   Symmetry about z axis

LIST OF SYMBOLS

E	Modulus of elasticity (Mpa)
G	Shear modulus of elasticity (Mpa)
I	Moment of inertia of a cross section
J	Torsional constant
I_w	Warping constant
v	Displacement in y-direction
w	Displacement in z-direction
θ	Angle of twist about x-axis
N	Shape matrix of a finite element
A	Area of cross section
Q	First moment of area of a cross section
Q_ω	First moment of warping
Bo	External boundary of a cross section
B1, B2, B3	Internal boundary of a cross section
a	Side length of a four node square finite element
C	Centroid of the cross section
O	Shear center of the cross section
F_x	Axial Force
M_Y	Bending moment about y axis of centroid
M_Z	Bending moment about z axis of centroid

V_Y	Transverse load in y direction
V_Z	Transverse load in z direction
T_s	Uniform Torque
T_w	Warping Torque
M_w	Bi-moment
σ_x	Normal Stress
τ	Shear Stress
σ_{VM}	Von Mises Stress
σ_e	Element Von Mises stress
σ_{min}	Minimum Von Mises stress value of the cross section
σ_{max}	Maximum Von Mises stress value of the cross section
σ_{lim}	Allowable(limit) Von Mises stress
ω	Warping function of a cross section for arbitrary point
ω^*	Warping function w.r.t shear center
Y_C	Y coordinate of cross-section centroid w.r.t initial coordinate axes
Z_C	Z coordinate of cross-section centroid w.r.t initial coordinate axes
Y_o	Y coordinate of shear center w.r.t centroid
Z_o	Z coordinate of shear center w.r.t centroid
q_y	Load intensity in y direction
q_z	Load intensity in z direction

N	Total element number
B	Gradient of shape matrix
Y_n	Y coordinate of nth element centroid w.r.t cross-section centroid
Z_n	Z coordinate of nth element centroid w.r.t cross-section centroid

CHAPTER 1

INTRODUCTION

With the development of computational power, a wide range of possible applications of optimization methods have become popular in the field of structural engineering. Size optimization, shape optimization, and topology optimization— which are the classes of structural optimization— can be applied in the early stages of the design process. While the optimum size and/or thickness of predefined members are determined by size optimization, the optimum shape is obtained by modifying the predefined boundaries of members. However, when it comes to topology optimization, the aim is to find the optimum shape and layout of cavities inside the design domain by not presenting any limits with predefined members or boundaries. Topology optimization is a good way to better understand the design domain and to investigate the best design options, especially during the conceptual design stages. Topology optimization does not supply the final structure design, rather, it helps to attain a rough idea regarding the most efficient topology. Hence, shape and size optimizations should be applied in the wake of topology optimization completion [1].
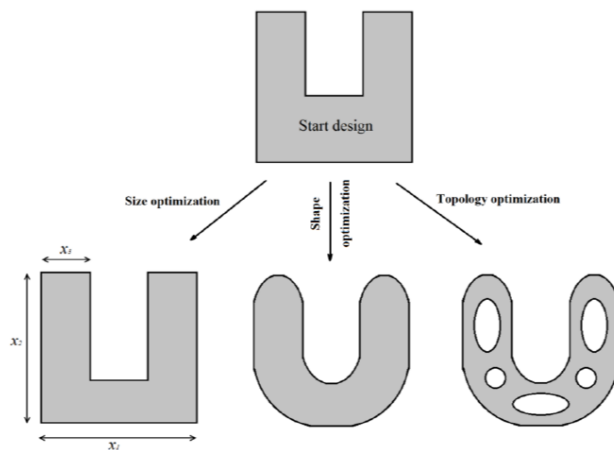
Figure 1.1. Structural Optimization Methods [2]

1

There are two popular design problems: namely, stress constrained weight minimization and volume constraint compliance minimization. The aim of the former is to minimize the volume fraction while satisfying stress constraints; whereas, the latter aims to maximize the stiffness for a given volume fraction[3].

In recent years, many topology optimization techniques have been produced in order to solve these two types of problems such as the optimality criteria method; the convex linearization method; the method of moving asymptotes and successive linear programming; and the Evolutionary Structural Optimization (e.g. ESO, BESO) methods [3].

According to critics and studies comparing optimization methods, the ESO method, developed by Xie and Steven [1][4], is the most popular and the simplest technique for topology optimization. This method focuses on the basic concept of gradually removing the inefficient material from the structure. The evolution of topology in ESO continues by only removing elements from the structure. It is not capable of element addition. As a result, the Bi-directional Structural Optimization (BESO) method was introduced by Querin et al.[5] in order to add and remove elements simultaneously. BESO is suitable for both stress and compliance optimization problems. Von Mises elemental stress is a criterion for applying the BESO concept to a stress problem. The elements that have the lowest von Mises stress are removed and void elements near the highest von Mises stress regions are switched on as solid elements in the respective BESO algorithm.

Beams are very significant structural elements as they play an important role in carrying load. Rotor blades of helicopters and large wind generators are two typical examples. Most of the previous studies in literature dealt with the optimization of a structure as a whole, i.e. 2D and 3D problems, by using structural optimization methods. Although there are several discussions regarding topology optimization of the beam along its span and in the literature, and although some methods have been tested, only limited studies have been conducted on cross-section optimization [6].

2

Besides, at present, the majority of studies related to cross-section optimization have focused on the shape optimization of the cross-section in which the shape of the boundary of the cross-section is considered as the design variable. Whereas, optimization studies on cross-section topology are not commonly found in the literature. Deciding the location and direction of stiffeners in a closed beam section is a critical problem for the design of a beam of a cross-section. The location of the stiffener in a closed beam section cannot be found by the shape optimization method, but it is possible by topology optimization of beam cross-section.

1.1. Objective of the Study

The objective of this study is to propose a novel optimization method to find the optimum topology of a Vlasov beam cross-section under static combined loading.

1.2. Structure of the Thesis

There are six chapters in this thesis. In Chapter 1, general information about topology optimization of the structure is provided. The motivation behind this study and a literature survey are provided in this chapter.

In the second chapter, similar studies related to cross-section optimization are investigated. Also, the current methodologies used for optimization are summarized in this chapter.

In the third chapter, the finite element formulation of Vlasov beams is derived and used for obtaining the load distribution along the axial direction of a Vlasov beam. For a given loading, normal force, lateral forces, bending moments, uniform torque, non-uniform torque, and bi-moments on each point on the beam are determined via specified finite element formulations. Also, a 2D finite element formulation for a cross-section analysis is derived in order to determine the cross-section properties and stresses on the point in question in the cross-section. Explanations of these formulations are provided in said chapter.

In Chapter 4, a detailed explanation of the optimization methodology used in this study is given. The optimization procedure is explained from the introduction of the problem to the termination of the optimization process.

Sample problems are solved by using the presented optimization methodology in this work. Results are given and comparisons are made in Chapter 5.

In Chapter 6, a summary of the study and a discussion about the results are given. Moreover, comments on future work are noted.

CHAPTER 2

LITERATURE SURVEY

In this chapter, a brief explanation of previous studies found in the literature related to cross-section optimization is provided. Many works can be found in the literature addressing cross-section optimization. While some studies focus on the shape optimization of a certain section, others give importance to the material distribution within the section using conventional heuristic methods.

A study conducted by Kim and Kim [7] is the earliest attempt to optimize beam cross-sections topologically. They developed a section topology optimization technique for elastic bodies instead of directly for beam structures [8]–[12]. The formulation of this method was given and applications on various practical problems were presented. It is proposed in said study to find the optimal cross-section configuration by minimizing the objective function which is a weighted sum of bending and torsional rigidities. The beam bending rigidity is based on the classical beam theory, on the other hand, the St. Venant torsion theory is employed for torsional rigidity. In their study, the effect of non-uniform torsion due to restrained warping on the cross-section is not considered in the optimization.

According to Liu et al. [13], beam cross-section properties have to be determined based on proper theory in the optimization process. The Euler-Bernoulli or the Timoshenko theory can be applied for the calculation of bending rigidity due to the assumption that a cross-section maintains in the same plane during deformation. Nevertheless, these theories are not valid for the determination of optimized cross-section properties if the shape of the cross-section is non-circular. As a result, non-circular types of cross-sections suffer from warping, out-of-plane displacements, and deformation couplings. In order to obtain the optimum topological configuration for a

cross-section, the material distribution is changed in the design domain [8], [10], [14]–[16]. Since the distribution may not be homogenous, the authors formulated the optimization algorithm based on anisotropic beam theory, including cross-section warping and deformation couplings, for minimizing the compliance of the beam.

Zuberi et al. [6] developed a topology optimization method which includes an extrusion manufacturing constraint. They aimed to determine the optimal topology of a beam cross-section under the action of different loading and boundary conditions (Figure 2.1). Load distribution varies along a section for different beam systems such as in modern bridges, crane girders, railway bridge girders rail tracks, etc. These types of systems need to have a constant cross-section along the axial direction. Classical beam theory linear finite element models are inadequate in investigating the effect of the load location and configuration on a cross-section topology as this theory is based on the assumption that the load is uniformly distributed along the section. On the other hand, when the topology optimization problems of beams requiring a constant cross-section are solved by using a solid finite element model the results give lattice or more complicated topologies of girder along the cross-section of the beam. Therefore, the authors suggest the extrusion constraint topology optimization method. The developed method was tested on the 3D model of the OptiStruct and Tosca for several loading and boundary conditions in order to find the optimal cross-section topologies. Compliance minimization is the focus of their optimization method; it is aimed to have uniform compliance history and convergent solutions at the end of the optimization process.
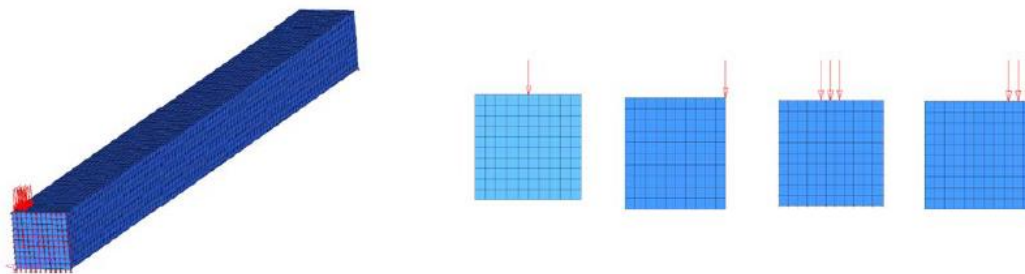
Figure 2.1. Representative Model of Beam and Different Load Cases [6]

6

In the study performed by Andelic et al. [17], optimization of a thin-walled open section Z beam subjected to bending and constrained torsion was addressed. The authors used the area of the cross section as an objective function for the "Z" shape beam. The stress of the type section is the stress constraint of their study and the Lagrange multiplier method is utilized to obtain the optimum dimensions of the Z beam. This study, therefore, addresses the problem of shape optimization. Similarly, in literature, the optimizations of different types of cross sections such as an I-section-section or a triangular section are performed with the Lagrange multiplier method.

The problem of finding an optimum cross-section of a beam subjected to various loading conditions is solved by using a Genetic Algorithm (GA) in the work conducted by Griffiths and Miles [18]. Their study seeks to explore the efficiency and effectiveness of a GA without direct guidance on how to solve the problem, especially for difficult design tasks.

Evolutionary Structural Optimization allows the use of different criteria. In the research presented by Proos [19] the moment of inertia is selected as the criterion and ESO is applied to maximize inertia. Unlike the material property of stiffness, the area moment of inertia has geometric properties. This means that the analysis of the inertia optimization of the cross-section does not depend on the loads on the beam or the constraints. This is the major differentiating aspect of the process introduced by Proos [19]. His process starts with the calculation of the moment of inertia of each element in the finite element model and the calculated MOI values are considered as the sensitivity of the element. These sensitivity numbers are then used by the optimization method to determine whether their respective elements are to be removed.

CHAPTER 3

FORMULATION

3.1. Determination of Stress Resultants on a Cross Section

In this study, optimization of the beam cross-section is performed by using stresses on the cross-section. In order to calculate stresses on the section, it is needed to know force and moment distribution on the beam. This chapter explains the methodology for determining the stress resultants at a given section.
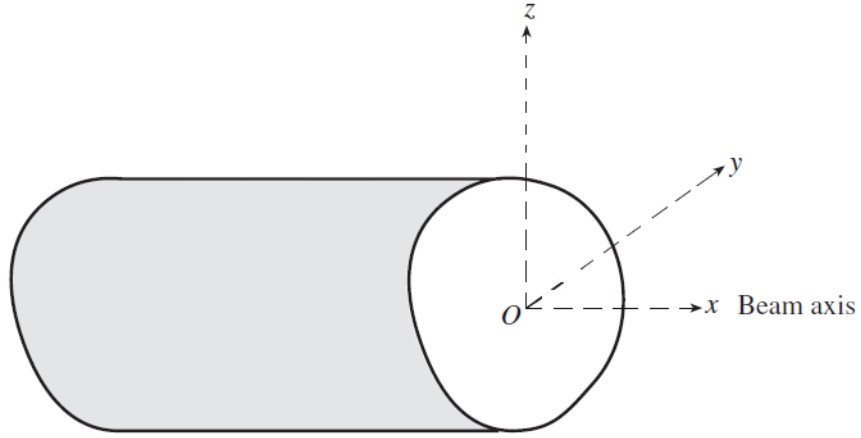
Figure 3.1. Coordinate System of a Beam

The governing equations of a beam are:

$$EA(u'' - \alpha \Delta T') = -f_x \tag{3.1a}$$

$$E\left(I_y I_z - I_{yz}{}^2\right)v^{\text{iv}} = I_y f_y + I_{yz} f_z \tag{3.1b}$$

$$E\left(I_y I_z - I_{yz}{}^2\right)w^{\text{iv}} = I_z f_z + I_{yz} f_y \tag{3.1c}$$

$$EI_w \theta^{\text{iv}} - GJ\theta'' = m_x \tag{3.1d}$$

where θ is the angle of twist, u, v, w and f_x, f_y, f_z are the displacements and the intensities of distributed forces in x, y, z directions, respectively, m_x is the intensity of the distributed torque, ΔT is the thermal force, E is the elasticity of modulus, G is the shear modulus, α is the thermal expansion coefficient of the beam material, A is the area, I_y, I_z, I_{yz} are the second moment of area, J is the torsional constant and I_w is the warping constant of the cross section.

Then, the stress resultants in a cross section are

$$F_x = EA(u' - \alpha\Delta T) \tag{3.2a}$$

$$M_y = EI_{yz}v'' - EI_y w'' \tag{3.2b}$$

$$M_z = EI_z v'' - EI_{yz} w'' \tag{3.2c}$$

$$M_w = EI_w \theta'' \tag{3.2d}$$

$$V_y = EI_{yz} w''' - EI_z v''' \tag{3.2e}$$

$$V_z = EI_{yz} v''' - EI_y w''' \tag{3.2f}$$

$$T_s = GJ\theta' \tag{3.2g}$$

$$T_w = -EI_w \theta''' \tag{3.2h}$$

$$T = T_s + T_w \tag{3.2i}$$

where F_x is the axial force, V_y, V_z are the shear forces, M_y, M_z are the bending moments, M_w is the warping moment(bi-moment), T_s is the St.Venant torque, T_w is the warping torque. T is the total torque acting on the cross section. The resultants are calculated either by solving the governing equations or by using a computational method. One of the choices in computational methods is the finite elements analysis. The resultants F_x, M_y, M_z, V_y, V_z are obtained by using the standard bar and Euler-Bernoulli beam finite elements. The resultants T_s, T_w, M_w can be obtained by a torsion finite element.

Torsion Finite Element

The weak form of the torsion equation is

$$\int g(EI_w\,\theta^{\mathrm{iv}} - GJ\theta'' - m_x)dx = 0$$

Where $g(x)$ is a test function. Using integration by parts, the weak form can be expressed as:

$$EI_w\int g''\theta''dx + GJ\int g'\theta'dx = (gT)_B + (g'M_w)_B + \int gm_xdx$$

The subscript B indicates the boundaries. Consider a finite element of length L with node-a at $x = 0$ and node-b at $x = L$ as

The twist angle θ can be assumed as

$$\theta = \boldsymbol{\Omega}\boldsymbol{\delta}$$

Where,

$$\boldsymbol{\Omega} = \frac{1}{L^3}[(L + 2x)(L - x)^2 \quad Lx(L - x)^2 \quad x^2(3L - 2x) \quad Lx^2(x - L)]$$

And

$$\boldsymbol{\delta} = \begin{bmatrix} \theta_a \\ \theta'_a \\ \theta_b \\ \theta'_b \end{bmatrix}$$

Let $\boldsymbol{G}$ be the vector of test functions. Using Galerkin method in which $\boldsymbol{G} = \boldsymbol{\Omega}$, the weak form can be written as

$$EI_w\int \boldsymbol{\Omega}''^T\boldsymbol{\Omega}''\boldsymbol{\delta}dx + GJ\int \boldsymbol{\Omega}'^T\boldsymbol{\Omega}'\boldsymbol{\delta}dx = (\boldsymbol{\Omega}^T T)_B + (\boldsymbol{\Omega}'^T M_w)_B + \int \boldsymbol{\Omega}^T m_xdx$$

Let

$$k_w = \int \boldsymbol{\Omega}''^T \boldsymbol{\Omega}'' \boldsymbol{\delta} dx \qquad (3.3a)$$

$$k_s = \int \boldsymbol{\Omega}'^T \boldsymbol{\Omega}' \boldsymbol{\delta} dx \qquad (3.3b)$$

$$f = (\boldsymbol{\Omega}^T T)_B + (\boldsymbol{\Omega}'^T M_w)_B + \int \boldsymbol{\Omega}^T m_x dx \qquad (3.3c)$$

Then, the element level equilibrium equation can be expressed as

$$[EI_w \boldsymbol{k}_w + GJ\boldsymbol{k}_s]\boldsymbol{\delta} = \boldsymbol{f}$$

Assembling the elements and imposing the boundary conditions, the nodal values of the twist angle θ can be determined. Then, the resultants T_s, T_w, M_w are computed as

$$T_s = GJ\boldsymbol{\Omega}' \boldsymbol{\delta} \qquad (3.4a)$$
$$T_w = -EI_w \boldsymbol{\Omega}''' \boldsymbol{\delta} \qquad (3.4b)$$
$$M_w = EI_w \boldsymbol{\Omega}'' \boldsymbol{\delta} \qquad (3.4c)$$

3.2. Calculation of Stresses over a Cross section

In this thesis, the normal and shear stresses acting on a cross section are determined by using the methodology in the study of Erdoğan [20]. This methodology has been modified for four node square elements, because it is easy to formulate and implement to the topology optimization method. Also, displacements and element geometry are specified by the same shape function.

3.2.1. Pure Bending and Normal Force

The section is discretized by N number of 4-node square finite elements having side length "a". All elements are firstly located in the arbitrarily selected initial coordinate system. After finding the centroid, the node locations are transferred to the centroid coordinate system (C_{YZ}).
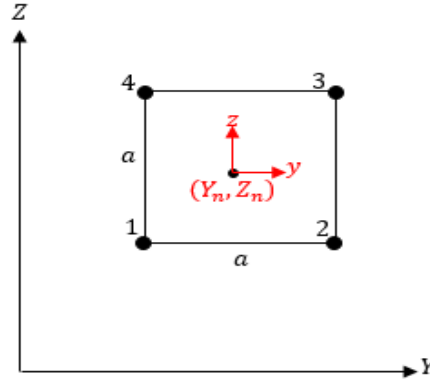
Figure 3.2. Four node Square Element of Cross Section

Total area of the section is found as

$$A = Na^2 \tag{3.5}$$

The second moment of areas of a section

$$I_Y = \sum_{n=1}^{N} a^2 \left(\frac{a^2}{12} + Z_n{}^2 \right) \tag{3.6a}$$

13

$$I_Z = \sum_{n=1}^{N} a^2 \left(\frac{a^2}{12} + Y_n{}^2 \right) \tag{3.6b}$$

$$I_{YZ} = -\sum_{n=1}^{N} a^2 Y_n Z_n \tag{3.6c}$$

Then, the normal stress at the centroid of the nth element due to axial force (F_x) and bending moments (M_Y, M_Z)

$$(\sigma_x)_e = \frac{F_x}{A} + \frac{1}{I_Y I_Z - I_{YZ}{}^2} [M_Y(Z_n I_Z + Y_n I_{YZ}) - M_Z(Y_n I_Y + Z_n I_{YZ})] \tag{3.7}$$

3.2.2. Transverse Loads

This section deals with the shear stresses resulting from transverse loadings. Finite element analysis is used to compute the shear stresses. Also, the location of shear center is discussed in this chapter.

Suppose that a cross-section in which Bo is external boundary and B1, B2, B3 are internal boundaries; transverse loads V_y and Vz are applied at the shear center (O) so that no twisting moment occurs.
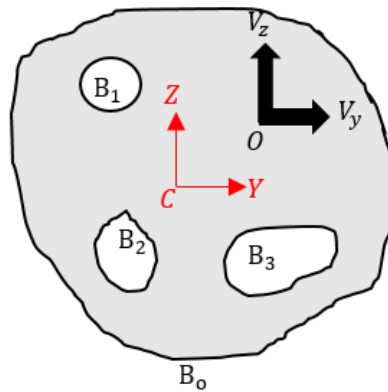
Figure 3.3. Representative View of external and internal Boundaries of cross-section

14

The first derivatives of the moments give the transverse loads as follows:

$$\frac{dM_y}{dx} = V_z \quad \frac{dM_z}{dx} = -V_y \tag{3.8}$$

Saint Venant assumed that the stresses σ_y, σ_z and τ_{yz} are negligibly small, leaving σ_x, τ_{xy} and τ_{xz} as unknown stresses. The normal stress σ_x for a beam undergoing pure bending is

$$\sigma_x = \frac{1}{I_y I_z - I_{yz}^2} \left[M_y \left(I_z Z + I_{yz} Y \right) - M_z \left(I_y Y + I_{yz} Z \right) \right]$$

With the assumption of that there are no body forces, the equation of equilibrium becomes

$$\frac{\partial \tau_{xy}}{\partial y} + \frac{\partial \tau_{xz}}{\partial z} = -\frac{\partial \sigma_x}{\partial x} = -\beta \tag{3.9}$$

Where,

$$\beta = \frac{1}{I_y I_z - I_{yz}^2} \left[\left(I_y V_y + I_{yz} V_z \right) \quad \left(I_z V_z + I_{yz} V_y \right) \right] \begin{bmatrix} Y_n + y \\ Z_n + z \end{bmatrix}$$

Let φ be a strain function such that

$$\tau_{xy} = \frac{\partial \varphi}{\partial y} , \tau_{xz} = \frac{\partial \varphi}{\partial z}$$

Then, the equilibrium equation is rewritten as

$$\nabla^2 \varphi + \beta = 0 \tag{3.10}$$

Next, multiplying governing equation by an arbitrary test function g and integrating over the entire domain using divergence theorem, the weak form is obtained.

$$\int_B g\, \vec{\nabla}\varphi \cdot \vec{n}\, ds - \int_A \vec{\nabla}g \cdot \vec{\nabla}\varphi\, dA = -\int_A g\beta\, dA$$

Due to the boundary condition $\vec{\nabla}\varphi \cdot \vec{n} = 0$ the first term of the left side is zero and the weak form is rewritten as follows:

$$\int_A \vec{\nabla}g \cdot \vec{\nabla}\varphi\, dA = \int_A g\beta\, dA$$

The function φ is approximated over each element by

$$\boldsymbol{\varphi} = \boldsymbol{N}(\boldsymbol{y}, \boldsymbol{z})\boldsymbol{\varphi}^e = [N_1 \quad N_2 \quad N_3 \quad N_4]\begin{bmatrix} \varphi_1 \\ \varphi_2 \\ \varphi_3 \\ \varphi_4 \end{bmatrix}$$

Where φ^e are the values of φ at the nodes of element e. $\boldsymbol{N}$ is the row vector of shape function for four node square element.

$$\boldsymbol{N} = [N_1 \quad N_2 \quad N_3 \quad N_4]$$

The two dimensional shape functions [21] are

$$N_1 = \frac{1}{4a^2}(a - 2y)(a - 2z)$$

$$N_2 = \frac{1}{4a^2}(a + 2y)(a - 2z)$$

$$N_3 = \frac{1}{4a^2}(a + 2y)(a + 2z)$$

$$N_4 = \frac{1}{4a^2}(a - 2y)(a + 2z)$$

Then, the gradient of shape matrix is obtained as

$$\boldsymbol{B} = \vec{\nabla}\boldsymbol{N} = \begin{bmatrix} \dfrac{\partial \boldsymbol{N}}{\partial y} \\[2mm] \dfrac{\partial \boldsymbol{N}}{\partial z} \end{bmatrix} = \begin{bmatrix} 2z - a & a - 2z & a + 2z & -a - 2z \\ 2y - a & -a - 2y & a + 2y & a - 2y \end{bmatrix}$$

Similarly assume test function g as $\boldsymbol{g} = N(y,z)g^e$. Then, the gradients of the functions are written as

$$\vec{\nabla}\boldsymbol{\varphi} = [\boldsymbol{B}][\boldsymbol{\varphi}] \text{ and } \vec{\nabla}\boldsymbol{g} = [\boldsymbol{B}][\boldsymbol{g}]$$

The weak form of the governing equations becomes

$$\int_A \boldsymbol{B}^T\boldsymbol{B}\ \varphi dA = \int_A \boldsymbol{N}^T\beta dA \tag{3.11}$$

The stiffness matrix of an element (k_e) is

$$k^e = \int_A \boldsymbol{B}^T\boldsymbol{B}\ dA = \frac{1}{6}\begin{bmatrix} 4 & -1 & -2 & 1 \\ -1 & 4 & -1 & -2 \\ -2 & -1 & 4 & -1 \\ -1 & -2 & -1 & 4 \end{bmatrix}. \tag{3.12}$$

The element force vector (f^e) is

$$f^e = \int_A \boldsymbol{N}^T\beta dA = \frac{a^2}{24(I_yI_z - I_{yz}{}^2)}\begin{bmatrix} 6Y_n - a & 6Z_n - a \\ 6Y_n + a & 6Z_n - a \\ 6Y_n + a & 6Z_n + a \\ 6Y_n - a & 6Z_n + a \end{bmatrix}\begin{bmatrix} I_yV_y + I_{yz}V_z \\ I_zV_z + I_{yz}V_y \end{bmatrix} \tag{3.13}$$

The global stiffness and force matrices are constituted to find the value of φ on each node by solving the below equation.

$$\boldsymbol{\varphi} = \boldsymbol{K}^{-1}\boldsymbol{F}$$

Then, shear stresses at the centroid of the element due to the shear forces are

$$\begin{bmatrix} \tau_{xy} \\ \tau_{xz} \end{bmatrix}_e = \frac{1}{2a}\begin{bmatrix} -1 & 1 & 1 & -1 \\ -1 & -1 & 1 & 1 \end{bmatrix}\begin{bmatrix} \varphi_1 \\ \varphi_2 \\ \varphi_3 \\ \varphi_4 \end{bmatrix} \tag{3.14}$$

The moment created by V_y and V_z about the centroid can be calculated from the shear stresses such that,

$$M_x{}^e = \int_A (\tau_{xz}Y - \tau_{xy}Z)dA = \int_A [-Z \quad Y]\begin{bmatrix} \tau_{xy} \\ \tau_{xz} \end{bmatrix} dA$$

When the above equation is solved for the element e of the moment, and summed for all elements in the domain it becomes

$$M_x = \frac{a}{2}\sum_{n=1}^{N} Y_n(-\varphi_1 - \varphi_2 + \varphi_3 + \varphi_4) + Z_n(\varphi_1 - \varphi_2 - \varphi_3 + \varphi_4)$$

Then the Y coordinate of shear center (Y_o) and the Z coordinate of shear center (Z_o) are calculated as

$$Y_o = M_x \text{ for } V_y = 0 \text{ and } V_z = 1 \tag{3.15a}$$
$$Z_o = -M_x \text{ for } V_y = 1 \text{ and } V_z = 0 \tag{3.15b}$$

3.2.3. Uniform Torque (Unrestrained Warping)

In pure torsion, the location of the axis of twist is of no consequence when calculating torsional stresses. The angle of twist of a section along the x-axis is θ. For a specific point A on the cross-section, the displacement in the y and z directions in the centroid coordinates axis is approximated by the following equations:

$$u_y \approx -zx\theta'$$
$$u_z \approx yx\theta'$$

where θ' is the angle of twist per unit length and is constant over the cross section. $x\theta'$ is the rotation of a section of the cross-section at a distance x. Coulomb's work shows that beams of a circular cross-section under pure torsion will only rotate while having no displacement axially (warping). For all non-circular cross sections, experimental results demonstrate that an axial displacement occurs and that this displacement is relatively constant throughout the beam [5]. This implies that axial displacement caused by torsion is governed by some function that is dependent on the y and z directions but independent of the axial (x) direction. As such, the axial displacement u_x is proportional to the angle of twist per unit length, and a function describing the out of plane warping of the cross-section, $\omega(y,z)$. The unknown function is referred to as the warping function, defined as:

$$u_x = \theta'\omega(y,z)$$

<u>Strain Displacement Relation</u>

$$\gamma_{xy} = \frac{\partial u_y}{\partial x} + \frac{\partial u_x}{\partial y} = \theta'\left(-z + \frac{\partial \omega}{\partial y}\right) \tag{3.16a}$$

$$\gamma_{xz} = \frac{\partial u_z}{\partial x} + \frac{\partial u_x}{\partial z} = \theta'\left(y + \frac{\partial \omega}{\partial z}\right) \tag{3.16b}$$

Stress-Strain Relation

$$\tau_{xy} = G\gamma_{xy} = G\theta'\left(\frac{\partial\omega}{\partial y} - z\right) \tag{3.17a}$$

$$\tau_{xz} = G\gamma_{xz} = G\theta'\left(\frac{\partial\omega}{\partial z} + y\right) \tag{3.17b}$$

The equations of equilibrium under no body force is

$$\frac{\partial\tau_{xy}}{\partial y} + \frac{\partial\tau_{xz}}{\partial z} = 0 \tag{3.18}$$

The equilibrium equation can be rewritten as:

$$\frac{\partial^2\omega}{\partial y^2} + \frac{\partial^2\omega}{\partial z^2} = 0$$

As in the previous case the Cauchy's relation must be satisfied. Such that,

$$\frac{\partial\omega}{\partial n} = \vec{\nabla}\cdot\vec{n} = \lambda$$

where,

$$\lambda = zn_y - yn_z$$

The above relation must be satisfied along all boundaries.

The weak form of the equilibrium equation is

$$\int_A \vec{\nabla}g \cdot \vec{\nabla}\omega\, dA = \int_B g\lambda\, ds \tag{3.19}$$

The integral on the left side of the above equation will lead to the elemental stiffness matrix. The function ω is approximated over each rectangular element by

$$\omega = N(y, z)\omega^e$$

The same shape functions as in paragraph 3.2.2 are used. Therefore, the same stiffness matrix for the element occurs.

The element force vector due to the boundary condition is formulated as

$$f^e = \int_B N^T \vec{\nabla}\omega \cdot \vec{n}\, ds$$

Let the element shown below be on the boundary.
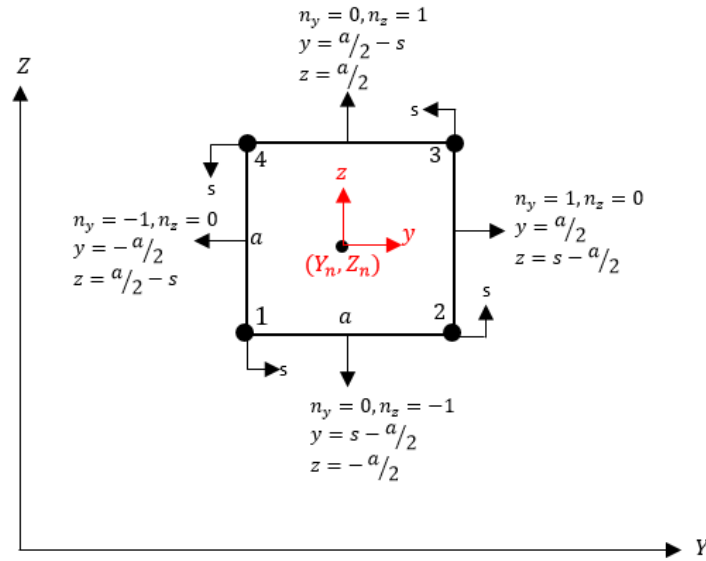
Figure 3.4. Four Node square Element Boundaries and Normal Vectors

For edge 1-2,

$$\{f^e\}_{1-2} = \int_0^a \frac{1}{4a^2} \, N^T_{1-2}(\vec{\nabla}\omega)_{1-2} \cdot (\vec{n})_{1-2} ds$$

When the integration is performed the force matrix yields for edge1-2 the following:

$$\{f^e\}_{1-2} = \alpha_b \frac{a}{12} \begin{bmatrix} 6Y_n - a \\ 6Y_n + a \\ 0 \\ 0 \end{bmatrix}, \alpha_b = \begin{cases} 0, & \text{if edge 1-2 is not on the boundary} \\ \\ 1, & \text{if edge 1-2 is on the boundary} \end{cases}$$

When the same calculations are made for the remaining edges, the corresponding force matrices are built up as follows:

$$\{f^e\}_{2-3} = \alpha_b \frac{a}{12} \begin{bmatrix} 0 \\ 6Z_n - a \\ 6Z_n + a \\ 0 \end{bmatrix}, \alpha_b = \begin{cases} 0, & \text{if edge 2-3 is not on the boundary} \\ \\ 1, & \text{if edge 2-3 is on the boundary} \end{cases}$$

$$\{f^e\}_{3-4} = \alpha_b \frac{a}{12} \begin{bmatrix} 0 \\ 0 \\ -6Y_n - a \\ -6Y_n + a \end{bmatrix}, \alpha_b = \begin{cases} 0, & \text{if edge 3-4 is not on the boundary} \\ \\ 1, & \text{if edge 3-4 is on the boundary} \end{cases}$$

$$\{f^e\}_{4-1} = \alpha_b \frac{a}{12} \begin{bmatrix} -6Z_n + a \\ 0 \\ 0 \\ -6Z_n + a \end{bmatrix}, \alpha_b = \begin{cases} 0, & \text{if edge 4-1 is not on the boundary} \\ \\ 1, & \text{if edge 4-1 is on the boundary} \end{cases}$$

The total force matrix of the element is the summation of these four matrices. Such that,

$$f^e = \{f^e\}_{1-2} + \{f^e\}_{2-3} + \{f^e\}_{3-4} + \{f^e\}_{4-1}$$

Then, the warping function values at the nodes of the element with respect to the centroid are found as:

$$\boldsymbol{\omega} = \boldsymbol{K}^{-1}\boldsymbol{F}$$

The torsional constant is given by [22]

$$J = I_Y + I_Z - \boldsymbol{F}^T\boldsymbol{\omega} \tag{3.20}$$

The shear stresses at the centroid of the element for a given uniform torque (T_s) are calculated as

$$\begin{bmatrix} \tau_{xy} \\ \tau_{xz} \end{bmatrix}_e = \frac{T_s}{J}\left(\left(\frac{1}{2a}\right)\begin{bmatrix} -1 & 1 & 1 & -1 \\ -1 & -1 & 1 & 1 \end{bmatrix}\begin{bmatrix} \omega_1 \\ \omega_2 \\ \omega_3 \\ \omega_4 \end{bmatrix} + \begin{bmatrix} -Z_n \\ Y_n \end{bmatrix} \right) \tag{3.21}$$

3.2.4. Non-Uniform Torque (Restrained Warping)

For restrained warping, the warping function with respect to the shear center (ω^*) is given in [22] as

$$\omega^* = \omega - Z_oY + Y_oZ - \frac{Q_\omega}{A} \tag{3.22}$$

The warping function value for each node is represented as

$$\boldsymbol{\omega}^* = \boldsymbol{N}(\boldsymbol{y},\boldsymbol{z})(\boldsymbol{\omega}^e)^*$$

23

Then, the first moment of the warping function for a given section is

$$Q_\omega = \sum_{n=1}^{N} \frac{(\omega_1 + \omega_2 + \omega_3 + \omega_4)}{4a^2}$$

The warping constant (I_w) with respect to the shear center is defined as the second moment of warping [22]. Such that,

$$I_w = \int_A (\omega^*)^2 \, dA$$

The same shape function is used, and then the warping constant yields

$$I_w = \frac{a^2}{9}\left(\omega_1^{*2} + \omega_2^{*2} + \omega_3^{*2} + \omega_4^{*2} + \omega_1^*\omega_2^* + \omega_2^*\omega_3^* + \omega_3^*\omega_4^* + \omega_4^*\omega_1^*\right) + \frac{a^2}{18}\left(\omega_1^*\omega_3^* + \omega_2^*\omega_4^*\right) \tag{3.23}$$

Let the shear stresses due to non-uniform torsion be $\tilde{\tau}_{xy}$ and $\tilde{\tau}_{xz}$, and the axial stress due to the effect of allowing the axial displacement be σ_x. Where,

$$\sigma_x = E\epsilon_x = E\frac{\partial u_x}{\partial x} = E\omega^*\frac{\partial^2\theta}{\partial x^2}$$

By choosing a strain function ϕ such that the stress states are:

$$\tilde{\tau}_{xy} = E\theta'''\frac{\partial\phi}{\partial y}$$

$$\tilde{\tau}_{xy} = E\theta'''\frac{\partial\phi}{\partial z}$$

The equilibrium equation becomes:

$$\frac{\partial \tilde{\tau}_{xy}}{\partial y} + \frac{\partial \tilde{\tau}_{xz}}{\partial z} = -\frac{\partial \sigma_x}{\partial x} = -E\omega^*\theta'''$$

By substituting the stress equations into the equilibrium equation, we get

$$\nabla^2\phi + \omega^* = 0 \tag{3.24}$$

Cauchy's relation is the same as the case in transverse load; the finite element methodology is also the same. Therefore, the weak form becomes:

$$\int_A \vec{\nabla}g \cdot \vec{\nabla}\phi dA = \int_A g\omega^* dA \tag{3.25}$$

Stiffness matrix does not change because the element shape matrices are identical.

The elemental force matrix is

$$\boldsymbol{f^e} = \int_A \boldsymbol{N^T}\omega^* dA = \frac{a^2}{36}\begin{bmatrix} 4 & 2 & 1 & 2 \\ 2 & 4 & 2 & 1 \\ 1 & 2 & 4 & 2 \\ 2 & 1 & 2 & 4 \end{bmatrix}\begin{bmatrix} \omega_1^* \\ \omega_2^* \\ \omega_3^* \\ \omega_4^* \end{bmatrix} \tag{3.26}$$

Then, strain function of each node is calculated by solving the equation below.

$$\boldsymbol{\phi} = \boldsymbol{K^{-1}F}$$

The shear stresses due to unrestrained warping are

$$\begin{bmatrix} \tilde{\tau}_{xy} \\ \tilde{\tau}_{xz} \end{bmatrix} = E\theta''' \begin{bmatrix} \dfrac{\partial \boldsymbol{\phi}}{\partial y} \\ \dfrac{\partial \boldsymbol{\phi}}{\partial z} \end{bmatrix} = E\theta''' \boldsymbol{B}\boldsymbol{\phi}^e = -\left(\dfrac{T_\omega}{2aI_w}\right) \begin{bmatrix} -1 & 1 & 1 & -1 \\ -1 & -1 & 1 & 1 \end{bmatrix} \begin{bmatrix} \phi_1 \\ \phi_2 \\ \phi_3 \\ \phi_4 \end{bmatrix} \qquad (3.27)$$

Bi-moment is defined in a fashion similar to the moment definition as

$$M_\omega = \int \omega^* \sigma_x dA = E\frac{\partial^2 \theta}{\partial x^2} I_w$$

The normal stresses at the centroid of the element due to warping are expressed as

$$(\sigma_x)_e = \frac{M_\omega}{I_w}\left(\frac{\omega_1^* + \omega_2^* + \omega_3^* + \omega_4^*}{4}\right) \qquad (3.28)$$

The stresses are found at the centroid of the all elements for different loading conditions. The summation of the corresponding stresses gives the total value of the individual stress state.

$$(\sigma_x)_e = (\sigma_x)_{PureMoment} + (\sigma_x)_{NormalForce} + (\sigma_x)_{NonUniform\,Torsion} \qquad (3.29\text{a})$$

$$\begin{bmatrix} \tau_{xy} \\ \tau_{xz} \end{bmatrix}_e = \begin{bmatrix} \tau_{xy} \\ \tau_{xz} \end{bmatrix}_{Transverse} + \begin{bmatrix} \tau_{xy} \\ \tau_{xz} \end{bmatrix}_{Unifor\,Torsion} + \begin{bmatrix} \tilde{\tau}_{xy} \\ \tilde{\tau}_{xz} \end{bmatrix}_{NonUniform\,Torsion} \qquad (3.29\text{b})$$

These stresses are converted to Von Mises stresses at the centroid of the elements as follows:

$$(\sigma_{VM})_e = \sqrt{(\sigma_x)_e^2 + 3\left((\tau_{xy})_e^2 + (\tau_{xz})_e^2\right)} \qquad (3.30)$$

CHAPTER 4

OPTIMIZATION METHODOLOGY

In this chapter, the methodology of the cross-section optimization process is explained. The main purpose of this study is to generate an algorithm to find the optimum topology of a cross-section with minimum weight that satisfies the stress constraints. It is to be obtained by changing the material distribution within the cross-section. During material distribution, it is needed to alter material status, i.e. from solid to void or from void to solid. In order to make such operations, a method, hereby proposed and named as the Evolutionary Growth Algorithm, has been developed as an optimization strategy.

The developed method, the Evolutionary Growth Algorithm, can be considered as a combination of the AESO and ESO methods, which were both explained in detail in the work conducted by Querin et al.[5]. In the Evolutionary Growth Algorithm, void elements near the highly stressed region are added and solid elements having low stress are removed starting from an initial guess.

The Evolutionary Growth Algorithm can be considered as a sort of Bi-directional Evolutionary Structural Optimization (BESO). It permits not only material removal, but also material addition at the same time, like BESO. In the BESO method, element addition and removal are decided according to the sensitivity number of the element and sensitivity number can be based on either the stress level or strain energy level of an element. However, it is noted that either selecting the stress level or strain energy level as the sensitivity number often gives similar topologies [4]. The Evolutionary Growth Algorithm, therefore, uses only Von Mises to define element sensitivity.

For most of the topology optimization problem, the design domain is the subdivided sections of the domain, which is an element of the domain. The design variable is the

property value of the element. Depending on the optimization method, the material property value can be discrete or continuous. In hard kill BESO method design, the variable can be only zero (0) or one (1), which defines the material presence. Whereas, in topology optimization methods like SIMP (which uses continuous intermediate element properties) and soft-kill BESO (which uses discrete intermediate element properties) use intermediate elements. Elements have a property value between zero and one. This means elements are not completely black or white, but they can be gray with respect to element properties.

In this thesis, the numbers 1 solid or 0 void, only denote the element property value. Hence, the element itself is the design variable of the optimization method used in this study. As an example, a simple variable denotation in the virtual cross section domain is given in Figure 4.1. The entire domain is divided by a 6x6 mesh. Vector "X" means that the design variables can be expressed as the matrix right of the figure.

$$X = \begin{bmatrix} 0 & 0 & 0 & 1 & 1 & 1 \\ 0 & 0 & 1 & 0 & 0 & 1 \\ 0 & 1 & 0 & 0 & 0 & 0 \\ 1 & 0 & 0 & 0 & 0 & 0 \\ 1 & 0 & 0 & 0 & 0 & 0 \\ 1 & 1 & 0 & 0 & 0 & 0 \end{bmatrix}$$
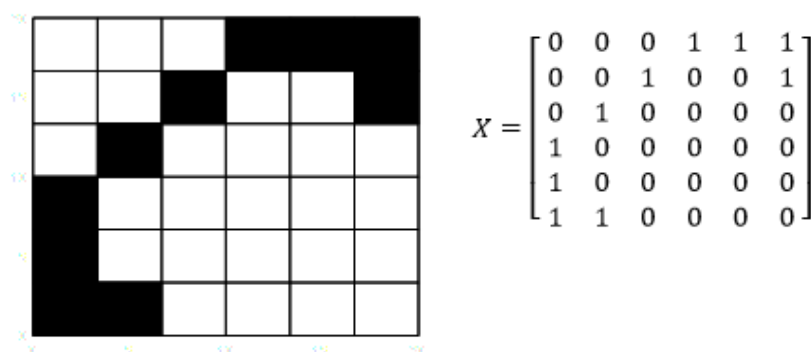
Figure 4.1. Example of Design Variable and Corresponding Matrix

Mean compliance minimization (stiffness maximization) or weight minimization can be selected as an objective function. In this study, the weight or area of the cross-section is minimized during optimization.

A predefined volume fraction is the convergence criteria of the current ESO/BESO method with von Mises stress objectives and stiffness optimization problems. Volume fraction or area ratio are not physical constraints of the structure and present different topologies depending on these values [23]. Therefore, for the Von Mises stress

objective, the maximum allowable stress limitation of the structure is used as a convergence criterion in this study.

The procedure defining the evolutionary optimization method used in this work is explained in the subsequent portion of this chapter.

4.1. Introduction of the Problem
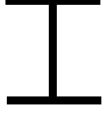
In this step, the material properties of the beam and locations of boundaries and forces are defined. The maximum available domain for the cross-section in question must also be specified in this step.

4.2. Definition of Design Constraints and Loading Points

Due to reasons related to manufacturing and efficiency, a structure with a constant cross-section is widely preferred in actual designs. Therefore, in this study, beams are assumed to have constant cross sections.

In some situations a structure with a symmetrical cross section is requested, which affects the optimization process. For this reason, this requirement is dealt with in this work as a design constraint. Before starting the optimization process, it is necessary to define any symmetric constraints if desired in the final topology. Table 4.1 shows the four symmetry constraints and corresponding section samples.

Table 4.1. *Examples of Beam Cross Sections with Symmetry Constraint*

	Symmetry Condition	Cross Section Example
1	Symmetry about z-axis,no symmetry about y-axis. (symy=0,symz=1)	
2	Symmetry about y-axis,no symmetry about z-axis. (symy=1,symz=0)	
3	Symmetry about both y and z axes (symy=1,symz=1)	
4	No symmetry about both y and z axes (symy=0,symz=0)	

The loading point of the cross-section is another constraint. In the research conducted by Zuberi et al.[6], the effects of various configurations and the location of the load and boundary conditions on the topology of beam cross sections are examined. In their study, the application points of loads on the section are fixed according to the fixed reference frame. In other words, the loading positions with respect to the shear center and centroid of the cross-section change during optimization. Unlike the approach of the authors, for the purpose of the research in this work, the external loads act such that,

1. Normal force (F_x) and transverse loads (V_y, V_z) pass through the centroid.
2. Normal force (F_x) is uniformly distributed over the cross section
3. Moment about x-axis (M_x) is free on the cross-section
4. Moments about the y and z planes contain the centroid
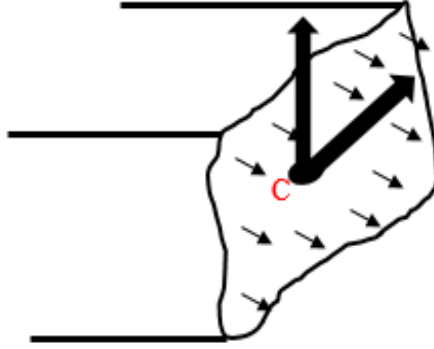
Figure 4.2. Normal (Axial) Force and Transverse Load Locations on a Beam

4.3. Selection of Optimization Criteria

In this study, the beam is assumed to have a constant cross-section. Optimization of a beam with a constant cross section depends not only on stress limitation, but also on the buckling response which is a very important phenomenon− especially in long beams. Therefore, the optimization of a beam under large compressive axial forces is not within the scope of this study. Furthermore, lateral torsional buckling is not taken into consideration in the present algorithm. Rather, the main purpose of the algorithm is to optimize the beam cross sections based on Von Mises stress levels, irrespective of the buckling characteristics of the section.

Element addition and the removal process is the most important part of evolutionary optimization. As mentioned above, Von Mises stresses are used as optimization criteria. The decision of which elements will be removed and added in the current iteration is made according to their respective Von Mises stress levels. In other words, the sensitivity of the element is nothing but its Von Mises stress.

4.4. Discretization of Cross Section

An entire cross-section domain is discretized by equally sized four-node square elements. The numbering of nodes and elements in the system starts from the bottom-left and proceeds, by row,-in the order shown in the figure below.
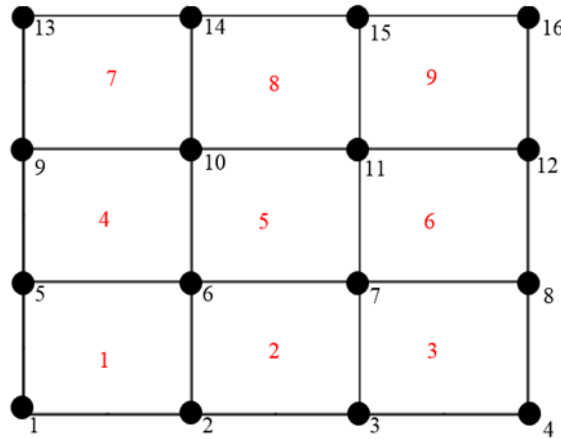
Figure 4.3. Numbering of Nodes and Elements for Cross Section Domain

The nodes of the elements and their coordinates are needed during the completion of FEA on a cross-section. Information regarding the element connectivity and node coordinates for the whole domain are generated and stored for use in the optimization process. Before starting said process, two matrices including element nodes and their coordinates are created. These are not affected by element addition and/or removal.

4.5. Selection of Initial Design

The initial design is the starting domain of the evolution of the structure. The optimization process starts its evolution from this domain. It can also be referred to as an "estimated initial design". It is decided according to engineering intuition and may vary according to the applied loading and constraints.

While deciding the initial design domain, the most important thing is that at least one element in the line of action of the lateral forces must be available in the initial domain.
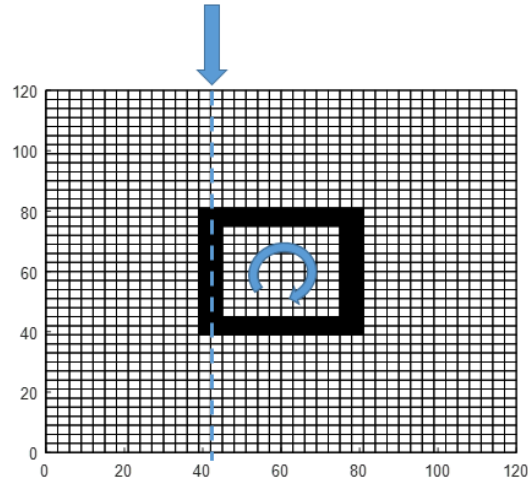
Figure 4.4. Example of an Initial Design Domain

4.6. Calculation of Cross-section Properties

Fundamental properties related to the cross-section of a given beam are necessary for the analysis of said beam. In this step, cross-section properties, area, the moment of inertia, torsional constant and the warping constant, are calculated by the FEA method described in Paragraph 2. These parameters are used in the next step for the computation of loads and moments on the beam.

4.7. Computation of Loads and Moments on the Beam

In this study, the optimization of a pre-selected cross section is performed. However, the warping stress resultants Mw and Tw are dependent on the cross-sectional shape. Therefore, a finite element analysis of the beam is necessary during the optimization process in which the cross-sectional shape is changed. After obtaining the new set of internal forces, the stresses in the section of interest are determined by using 2D finite element analysis.
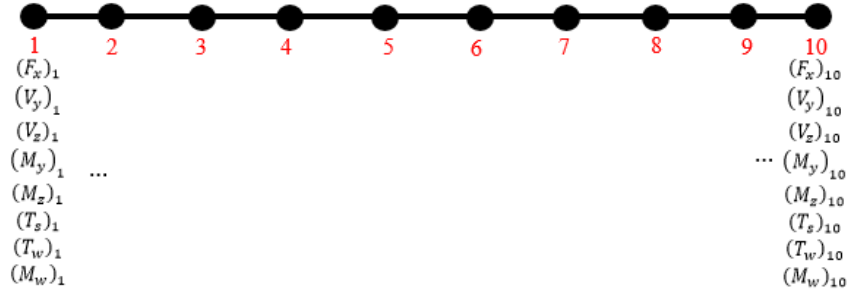
Figure 4.5. Calculated Loads and Moments on 1D element nodes

4.8. Finite Element Analysis on the Cross Section

Finite element analysis is carried out on a 2D cross-section in order to determine the Von Mises stresses of each element under the loads defined previous step. The formulation for finding stresses on the cross-section is given in Paragraph 3.2.

4.9. Element Addition and Removal

The procedure used for determining which elements are to be added and which ones are to be removed is explained herein. The cross-section domain may have regions that are heavily under-stressed and over-stressed. Material needs to be added to over-stressed regions and removed from under-stressed regions. The processes of element addition and removal are treated separately.

4.9.1. Element Addition Procedure

Element addition denotes the introduction and/or the reintroduction of elements into an evolving structure.

The addition of elements around highly stressed elements conduces the diffusion of stresses to newly introduced elements. This will reduce the maximum stress. Then, the maximum stress occurs at the other elements surrounding its previous location, but in a lessoned form.

Assume the element "e" is in the current domain and has the highest stress. Element e has three free edges and is attached to the structure by edge 1 as can be seen in Figure

4.6. Elements can be added to the structure from the free edges 2, 3 and 4.However, in order to fully diffuse the stress to the surrounding area elements that have adjoining nodes to the highest stressed element are also injected. After adding elements, the final area around element e would look as depicted in Figure 4.7.
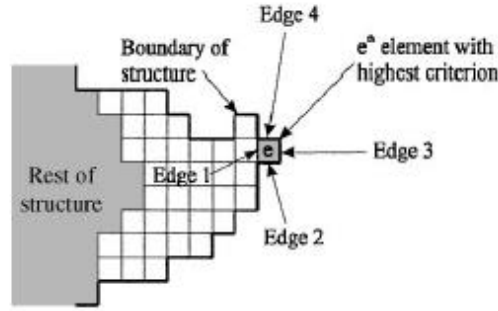
Figure 4.6. Element "e" on Boundary of a Cross Section Exhibiting Highest Stress [24]
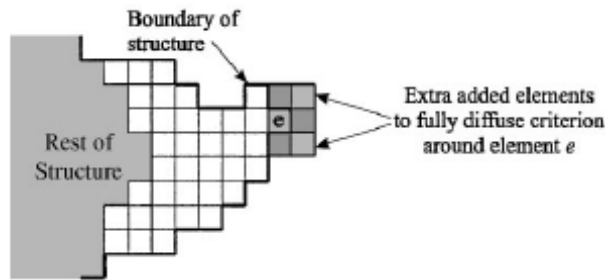
Figure 4.7. Added elements around Element "e" [24]

Elements are added to all free nodes and edges of elements satisfying Eq.(4.1). In addition to these elements, if there is a symmetry constraint in the problem; elements with respect to symmetry about the centroid of the domain are also added in the same manner. Such that,

$$\sigma_e > IR\ \sigma_{max} \tag{4.1}$$

where, σ_e is the element's Von Mises stress, and σ_{max} is the maximum Von Mises stress of the current design.

IR is an injection ratio. It restricts the number of elements to be added in one iteration. Moreover, the continuation of the optimization process is provided with the help of the injection ratio. The idea and formulation of the inclusion rate are compiled from the study of Querin et al. [5]. The general form of the inclusion rate is

$$IR = i_0 - i_1\, SS - i_2\, ON \tag{4.2}$$

where $0 \leq IR \leq 1$

i_0, i_1 and i_2 are the coefficients of the inclusion rate and they are determined from numerical experiments and the literature. It is observed that using higher values for i_0 works better in complex problems in terms of convergence.

Increasing the inclusion ratio diminishes the number of elements to be added in one iteration, or vice versa. Therefore, these coefficients can be varied for different optimization problems. SS and ON are the steady state number and oscillatory number, respectively. Detailed information about these numbers are given in 4.10.

4.9.2. Element Removal Procedure

Respectively less stressed elements are removed from the structure in each iteration. Like in the addition process, the number of elements to be removed from the domain is controlled.
Which elements to be removed are determined by the formula below:

$$\sigma_e < \sigma_{min} + \frac{(\sigma_{max} - \sigma_{min})}{RC} \tag{4.3}$$

If the symmetry constraints are available, elements satisfying the above equations and their symmetric elements are removed from the structure. RC is the removal constant specifying the reduction rate. As opposed to IR, RC does not change during optimization. By using this number, the decision of how many elements are to be removed in one iteration can be made. The greater the number, the fewer the elements

are cleared from the structure in one iteration or vice versa. Through this body of work it was determined that selecting this number between 10 and 20 gives satisfactory results.

The most critical issue of the removal process is that the coherent of the cross-section has to be maintained throughout the optimization process. No structural islands will be present in the final topology[24], i.e. all parts of the structure are connected to the main structure. A connectivity check algorithm is created to guarantee that all active elements are connected during each iteration. This is achieved by checking that all active elements (elements having a property value of 1), kept in design domain are connected to another element with at least one adjoining node. Hence, removing the element from the domain is supplied as the set of rules described below:

- Identify elements having stress less than the prescribed limit defined by Eq.(4.3).
- Sort of these elements in ascending order
- Remove each element one by one and check whether the removal of this element destroys the cross-section integrity or not. If this is not the case, i.e. the structure remains coherent, then this element is removed, on the other hand, if a disconnection occurs, this element is not removed.
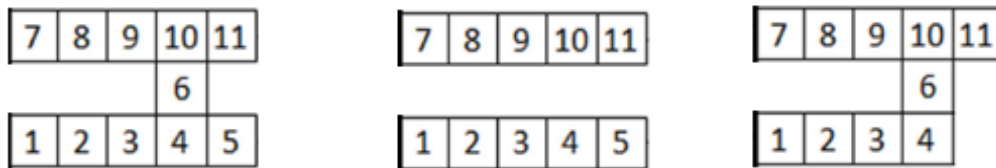

Figure 4.8. Illustration of Connectivity of Elements

For example, at any time of the optimization iteration assume the structure takes the form as in the left scheme in Figure 4.8. In that configuration, the structure is coherent. Assume elements 5 and 6 satisfy the inequality of eq.3.3, and so they need to be removed. When element 6 has been removed the two bar structure

occurs and connectivity is broken (in the middle of Figure 4.8.Therefore, it is not removed from the structure. If the same approach is applied to element 5, as in the scheme on the right in Figure 4.8, the removal of element 5 does not result in any connectivity problems and so it can be cleared.

- The previous item is repeated for all elements listed as under-stressed elements.

4.10. Steady State and Oscillatory State Check

IR depends on two factors; the first one is the steady state number .If there are no free elements around the elements satisfying the equation listed in Eq.(4.1), it means that there are no more elements to be added. Optimization can only continue by removing the elements which cause the maximum stress of the section from converging to the prescribed limit,. The proceeding of the addition process is enabled by increasing the steady state number (SS). This number is incremented by 1 until at least one element is found to be added. The second factor is the oscillatory state number (ON), which is an indicator of the oscillation state and occurs when the same elements are added and removed in the subsequent iterations. The oscillatory state is obtained by observing the area of the section in each iteration. If change of the area over the last 10 iterations is acceptably small (less than 0.001), and the stress limit has not been reached yet, the section is considered to be in an oscillatory state. Incrementing this number by 1 shifts the optimization process from the current state. This allows optimization to continue.

As such, the general form inclusion rate is formulated as

$$IR = i_0 - i_1\ SS - i_2\ ON \tag{4.4}$$

Where, i_0, i_1 and i_2 are the coefficients determined from the numerical experiments and can vary for different optimization problems.

Eq. (4.5) is used to check whether the optimization is in oscillatory state.

$$Change\ in\ area = \frac{\left|\sum_{i=1}^{5} Area_{k-i+1} - \sum_{i=1}^{5} Area_{k-i-4}\right|}{\sum_{i=1}^{5} Area_{k-i+1}} \tag{4.5}$$

4.11. Termination of Optimization and Fine-Tuning Process

The cycle of finite element analysis of a cross-section and element addition and removal continues until stress in the domain reaches the stress limit. The optimization process stops its evolution when the following convergence criterion, defined in terms of the difference between stress limit and domain stress, is satisfied.

$$\frac{|\sigma_{Max} - \sigma_{lim}|}{\sigma_{lim}} \leq 0.01 \tag{4.6}$$

σ_{Max} is the maximum Von Mises stress of an element in the structure and σ_{lim} is the prescribed stress limit related to beam material.

The objective is to obtain the minimum weight design with the maximum stress as close as to the stress limit as possible. During the optimization process, a group of elements are added and removed; however, this does not provide a good solution when the stress of the domain approaches the limit. After a stress point, it is needed to perform element addition and removal process sensitively. In order to perform such an operation a fine-tuned algorithm is generated which aims to obtain a more precise solution.

The fine-tuning of the algorithm proceeds similarly to the normal addition and removal process described in Paragraph 4.9. The only difference is the number of removed elements. If the maximum stress level is less than 99% of the allowable stress limit, then the fine-tuning method is utilized as follows:

$$\sigma_{Max} \leq 0.99\sigma_{lim} \tag{4.7}$$

1. The elements are sorted in ascending order according to the elemental stress value. The first element has minimum stress and the last element has maximum stress.

2. The first element and its symmetric elements (if a symmetry condition is pointed out) is selected

3. Elements found in the previous step are removed and the remaining domain is checked in terms of the connectivity of whole domain.

4. If the domain is still coherent after the removal process (the previous step) then the finite element analysis is performed and the stresses of new elements are calculated. If it is no longer coherent, then this element is reintroduced to the structure and the second element is selected.

Step 2 to 4 is repeated until the maximum stress is in the allowable range (convergence criterion defined in Eq. (4.6)).

The generalized flowchart of the optimization method used in this body of work can be represented as shown in Figure 4.9.
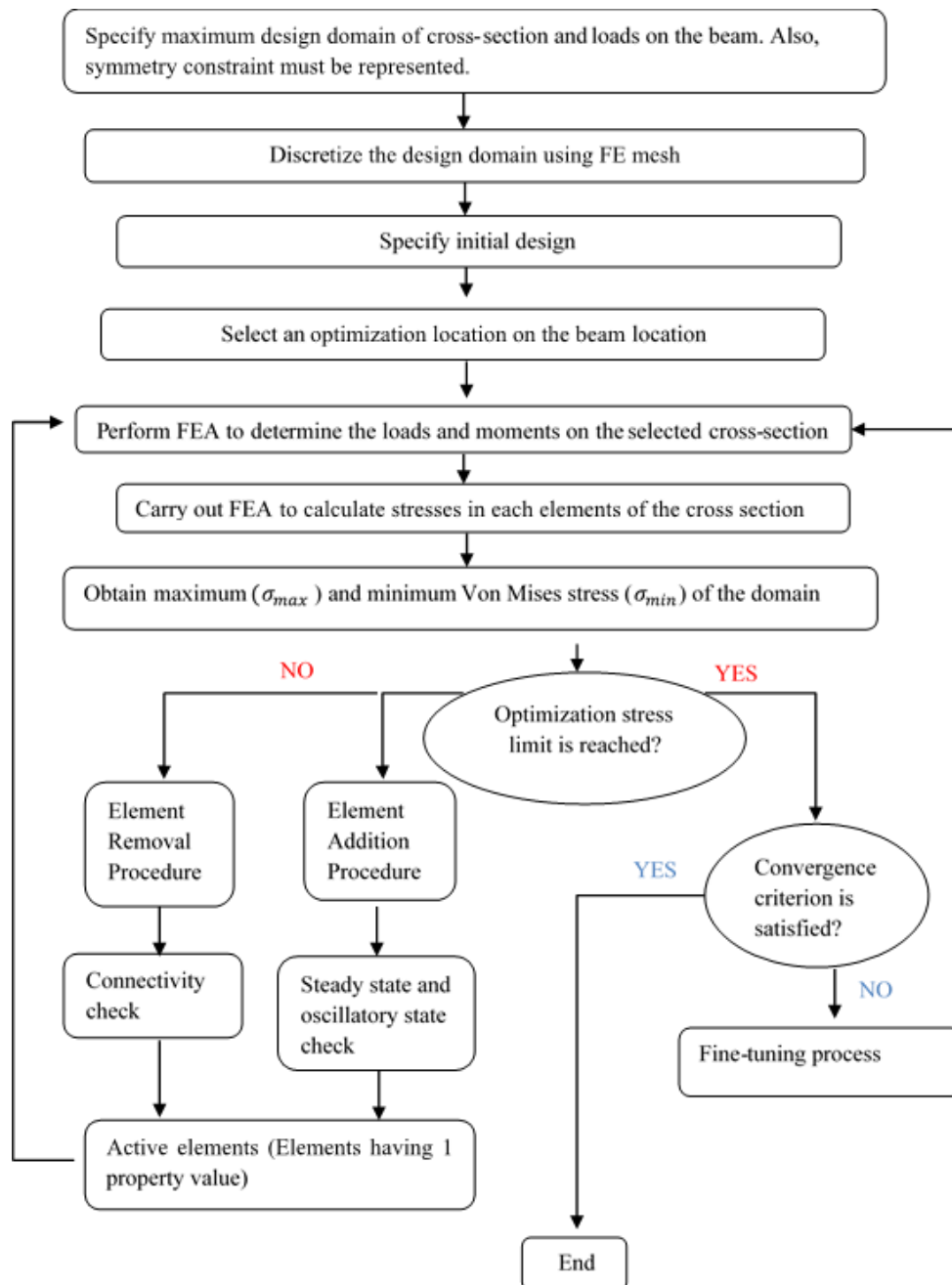
Figure 4.9. Flow Chart of the Optimization Process

CHAPTER 5

CASE STUDIES

In this chapter, to verify the optimization method presented in this work, representative numerical problems are handled. Cantilevered beams under different loading conditions are selected as case studies in order to solve and compare the results. In all of the case studies, it is aimed to find the optimum topology of the beam with a minimized weight while satisfying the stress limitation. The final topology of the presented method highly depends on the input parameters such as the magnitude and direction of the loads, initial design and element inclusion rate, etc. as explained in the previous section. In order to investigate the effects of these parameters on the final topology, different setup parameters are used for the same problems. In this way, discussion about the overall effectiveness can be made. For all of the examples, the possibility of buckling is not included.

5.1. Case Study 1

The first problem is to examine the optimum cross-section topology of the cantilevered beam under only a vertical concentrated load at the tip of the beam. The whole area of the cross-section domain is a 20x20 mm^2 square region. The length of the cantilevered beam is 100 mm. The allowable stress limit for the beam material used in the optimization algorithm is 250 MPa. Young's modulus and shear modulus are taken as 200 GPa and 80 GPa respectively.
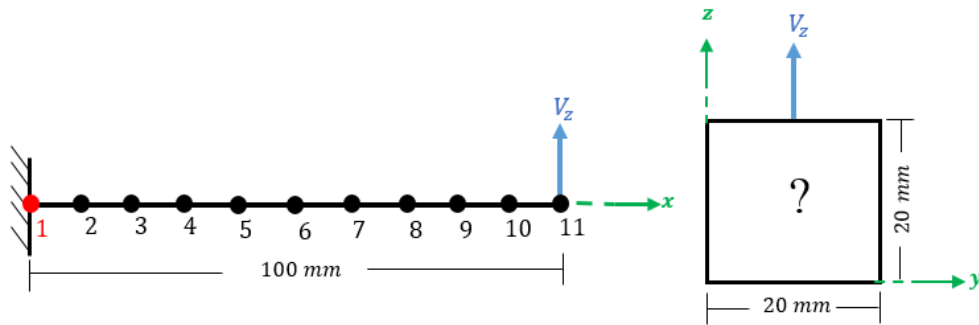
Figure 5.1. Force and Boundary Illustration of Problem 1

Figure 5.1 shows the representative graphical illustration of the problem. The beam is subdivided into 10 elements along the axial direction using 11 nodes. This is sufficient to calculate the stress resultants on each node. As mentioned in Chapter 4, stress analysis and optimization are only made on the node where optimization will be performed. The most critical location of this beam is the fixed endpoint due to the high bending moment. Therefore, the 1st node, shown in red in the figure above is considered as the optimization location of this problem.

The symmetry design condition is one of the most critical constraints, influencing the evolution of the optimization. In this problem, it is stated that the final topology has to be symmetric about the z-axis of the centroid. The required information for Problem 1 is summarized in table.

Table 5.1. *Specification of Problem 1*

Load	Location of Load	Max. Stress Limit	Symmetry Constraint	Optimization Location
Vertical Point Load (V_z)	At the free end	250 MPa	(symy=0,symz=1)	the fixed end

Optimization Run

At this stage, the Evolutionary Growth Algorithm has been run only once for the setup parameters listed below.

- Load values: $V_z = 1.0 \, kN$
- Initial design: Four elements in the middle of the domain (Figure 5.2)
- Element addition and removal formula: $IR = 0.95 - 0.01 \, SS - 0.1 ON$ and $RC = 10$
- Meshing: 60x60 mesh (i.e. 3600 elements)

The I-shape cross-section is the optimal topology for this problem as shown in Figure 5.2. At the beginning of the process, the initial domain is very small, which causes very high stress. By adding elements to highly stressed regions and removing the lesser-stressed elements, the area of the domain is increased and the maximum stress is reduced. Owing to the presence of the symmetry constraint, the final topology is symmetric about the z-axis.
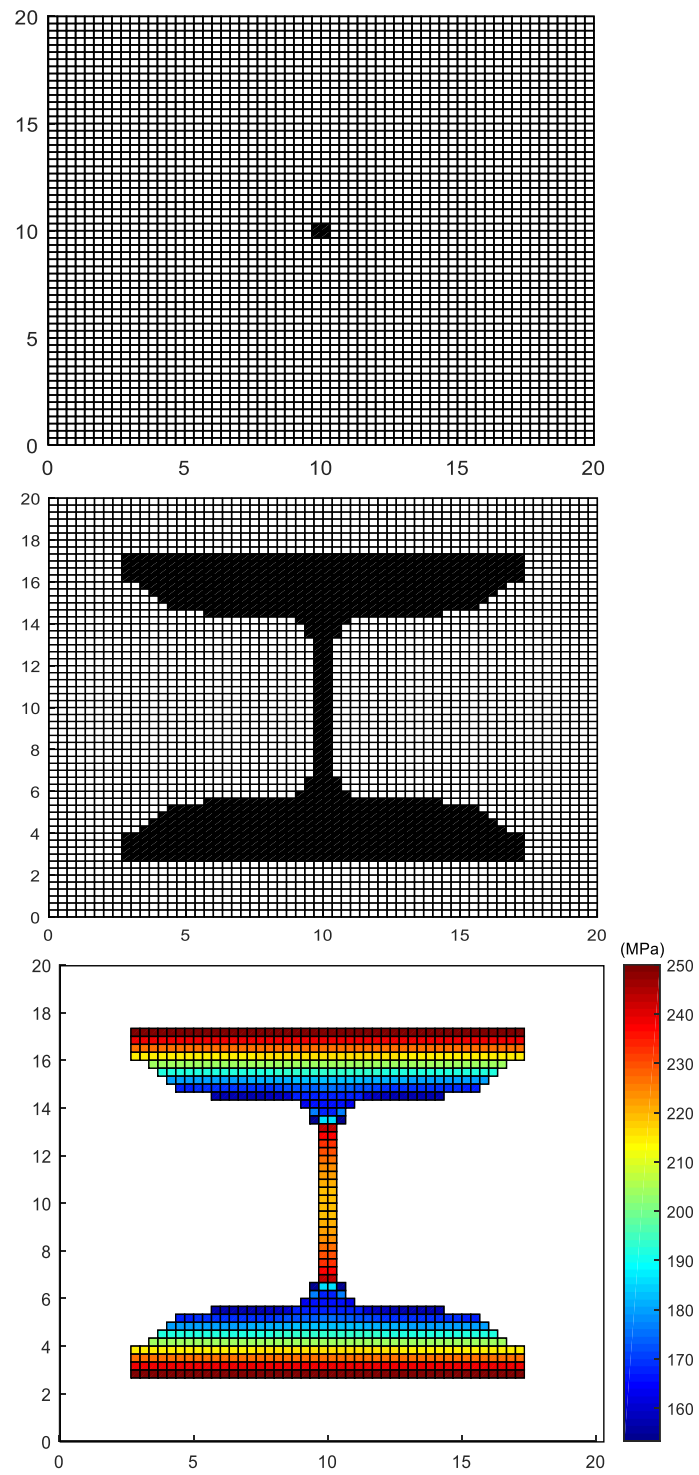
Figure 5.2. Optimization Run for Problem 1: Initial Design Domain (Top), Optimized Cross-section (Middle), Von Mises Stress Distribution (Bottom)

The process is terminated at the 39th iteration when the maximum stress stabilizes around 250 MPa, as can be seen from Figure 5.3, which indicates the change of area and maximum stress. At the 21st iteration, the maximum stress level is less than the prescribed limit, yet the difference between the maximum Von Mises stress and the allowable stress limit has not reached the convergence criterion limit. Therefore, after this iteration, elements are only removed from the structure one by one in order to increase the maximum stress slowly up to the stress limit (this is the fine-tuning process).
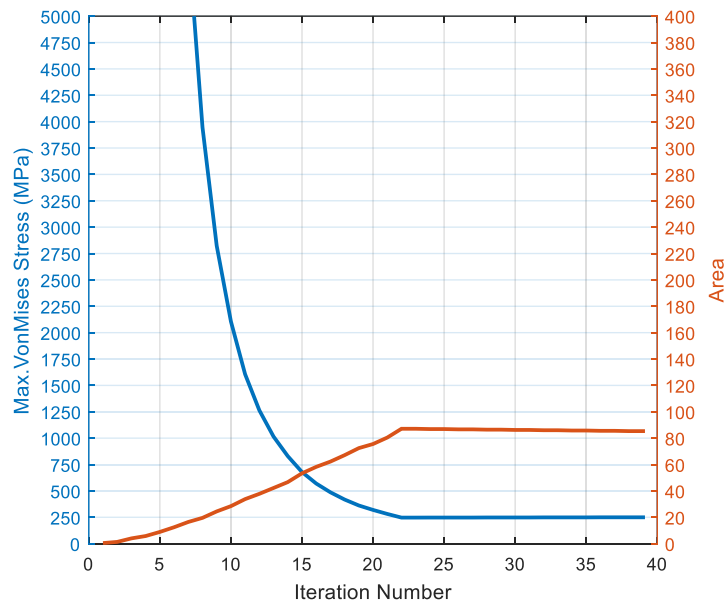
Figure 5.3. History of Maximum Stress and Area of Optimization Run for Problem 1

Shear center and applied force are always in the same line of action which results in the vertical force not creating any torque about the x-axis. Therefore, only the bending moment and vertical force occur throughout the beam. The driving loading in the cross-section that affects the stresses is the bending moment in this example; therefore, it is easily seen that stresses increase as the distance from the center increases;. This coincides with classical beam theory. Also, in the web of the found section is fully stressed as can be seen in Figure 5.2 in which bottom figure shows the Von Mises stress distribution over the optimized section.

The summary of the results are tabulated below.

Table 5.2. *Results Summary of the Optimization Runs for Problem 1*

Run	Loading	Initial Design	Final Topology	Area	Max. Von Mises Stress
1	$V_z = 1.0\ kN$	4 elements in the middle	"I" shape Cross Section	85.3 mm^2	249.7 MPa

Cross-section geometric properties of the obtained topology are listed in Table 5.3.

Table 5.3. *Geometric Properties of Identified Cross Sections for Problem 1*

Run	Second Moment of Areas			Torsional Constant	Warping Constant	Shear Center w.r.t centroid	
-	I_{yy} (mm^4)	I_{zz} (mm^4)	I_{yz} (mm^4)	J (mm^4)	I_w (mm^4)	Y_o (mm)	Z_o (mm)
1	2873	1159	0	204.8	36645	0	0

In the work conducted by Ishii and Aomura [25], the same problem was handled and solved via 3D frame based unit elements. Figure 5.4 shows the topology obtained by Ishii and Aomura for stiffness maximization with 36% volume constraint. The final topology is very similar to the one found by the presented method in this thesis.
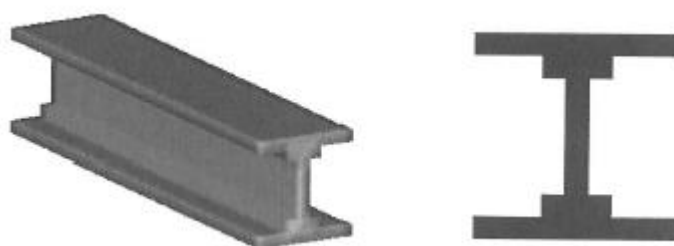
Figure 5.4. Optimum Cross-section Obtained by Ishii and Aomura [25]

When the identified topology is compared to the solution found by Zuberi et al. [6] , a similar topology is once again observed. In their study, a 3D beam model with the lowest compliance criterion is used.
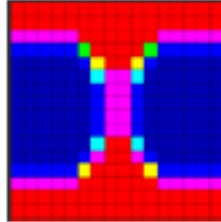
Figure 5.5. Result Found by Zuberi et al. [6] for Problem 1

5.2. Case Study 2

The second example is the analysis of cantilevered beam subjected to two transverse loadings at the tip of the beam.
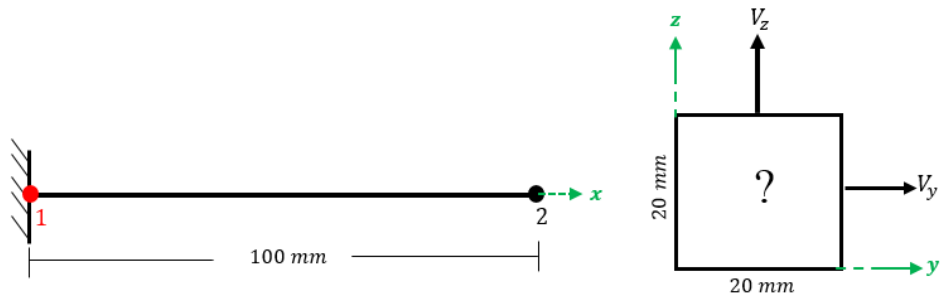
Figure 5.6. Force and Boundary Illustration of Problem 2

In this example, only one element is used to evaluate loads and moments. Transverse loads in the z and y directions are exerted at the second node of the beam. The section of the first node at the fixed end is the optimization location. The optimization algorithm computes the stresses and decides the element status based on the loads and moments on that node.

The beam properties, maximum allowable cross section domain, the number of elements and initial design domain are identical with the ones in Problem 1. Unlike the first case study, no symmetry condition is considered for this problem.

Table 5.4. *Specifications of Problem 2*

Load	Location of Load	Max. Stress Limit	Symmetry Constraint	Optimization Location
Vertical Point Load (V_z)	At the free end	250 MPa	(symy=0,symz=0)	the fixed end
Horizontal Point Load (V_y)				

<u>***Optimization Run 1***</u>

The first optimization run is performed with the following setup parameters:

- Load values: $V_z = 1.0 \ kN$ and $V_y = 1.0 \ kN$

- Initial design: Four elements in the middle of the domain (Figure 5.7)

- Element addition and removal formula: $IR = 0.9 - 0.01 \ SS - 0.1 ON$ and $RC = 10$

- Meshing: 60x60 mesh (i.e. 3600 elements)

Positive vertical load at the tip of the beam creates a negative bending moment, on the other hand, this is opposite of the situation for the horizontal load. In the first quadrant, these bending moments create normal stress in tension and in the fourth quadrant they cause compressive normal stress of equal magnitude. Then, the maximum stresses are formed in these areas. Therefore, elements have been added to the first and fourth quadrant of the section in order to diffuse the stress.

At the end of the optimization process a topology similar to the one in the first problem is obtained. It resembles an "I" type cross section rotated 45° about the centroid, which is the angle of resultant force vector.
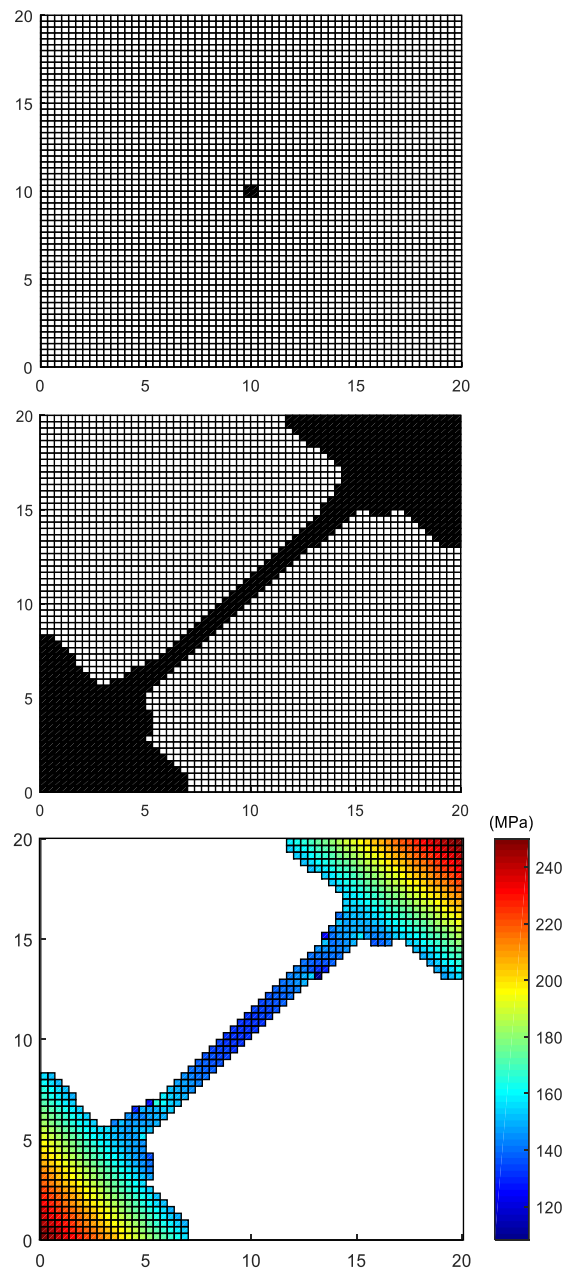
Figure 5.7. Optimization Run for Problem 2: Initial Design Domain (Top), Optimized Cross Section (Middle), Von Mises Stress Distribution (Bottom)

As seen the figure below,which shows the evolution history of maximum stress and section area, the rate of change of these two properties is very high at the beginning of the process. It slows down in subsequent iterations and maximum stress convergesthe the desired level.
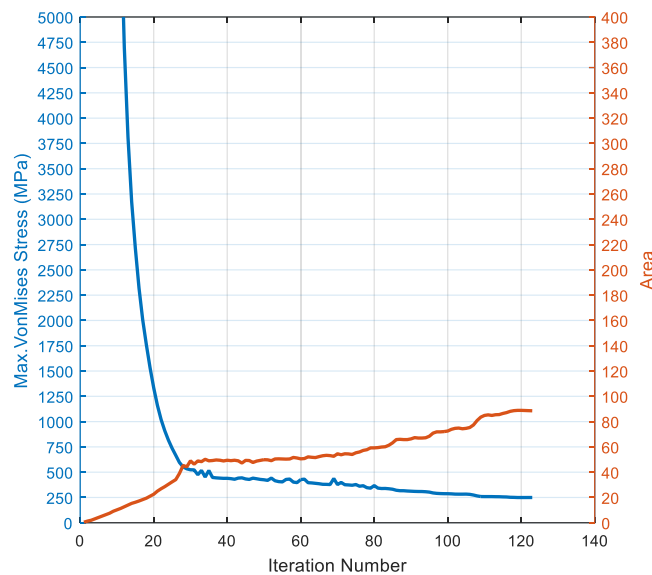
Figure 5.8. History of Maximum Stress and Section Area of Optimization Run for Problem 2

Optimization Run 2

The optimization is repeated with the reduced loads in the second run.

- Load values: $V_z = 0.5\ kN$ and $V_y = 0.5\ kN$
- Initial design: Four elements in the middle of the domain (Figure 5.9)
- Element addition and removal formula: $IR = 0.65 - 0.01\ SS - 0.1ON$ and $RC = 10$
- Meshing: 60x60 mesh (i.e. 3600 elements)
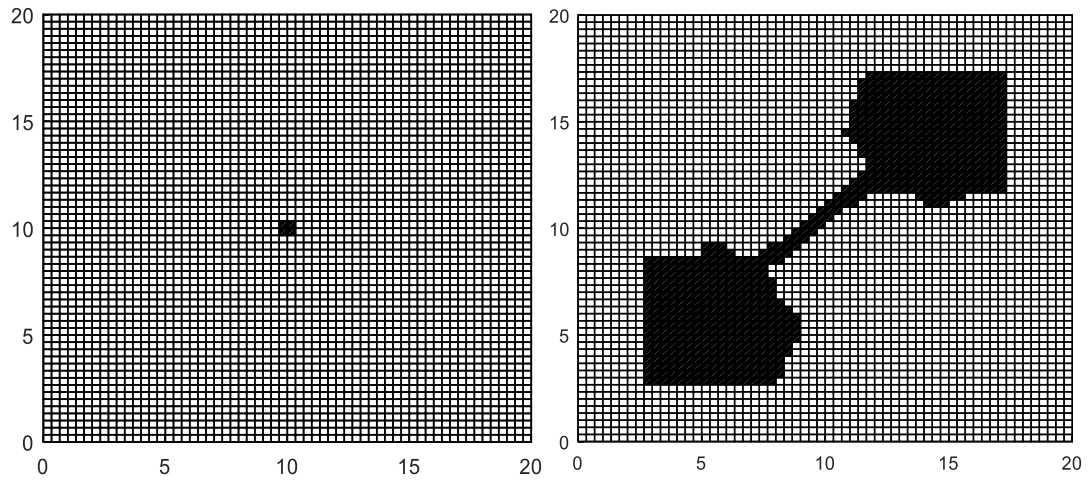
Figure 5.9. Optimization Run 2 for Problem 2: Initial Design Domain (Left), Optimized Cross Section (Right),

When half of the load values in the first run are applied, the final topology has not touched any boundary. The optimization process ends up with the topology satisfying design requirement as shown in Figure 5.9. The results of the first and second optimization runs proves that the final topology depends on the magnitude of the applied loads.

Finally, the obtained cross-section properties under the loads and boundary conditions specified for this example are tabulated below.

Table 5.5. *Results Summary of the Optimization Runs for Problem 2*

Run	Loading	Initial Design	Final Topology	Area	Max. Von Mises Stress
1	$V_z = 1.0\ kN$ $V_y = 1.0\ kN$	See Figure 5.7	See Figure 5.7	88.56 mm^2	249.7 MPa
2	$V_z = 0.5\ kN$ $V_y = 0.5\ kN$	See Figure 5.9Figure 5.7	See Figure 5.9	74.33 mm^2	247.3 MPa

Table 5.6. *Geometric Properties of Identified Cross-sections for Problem 2*

Run	Second Moment of Areas			Torsional Constant	Warping Constant	Shear Center w.r.t centroid	
-	I_{yy} (mm^4)	I_{zz} (mm^4)	I_{yz} (mm^4)	J (mm^4)	I_w (mm^4)	Y_o (mm)	Z_o (mm)
1	4124	4129	-3750	306	39825	-0.35	0.33
2	1560	1560	-1345	348	8198	-0.43	0.34

5.3. Case Study 3

In the third problem, the same beam as in the first problem is used. However, the loading type is different. The optimum cross-section topology is sought for when only a twisting moment is applied at the free end of the beam.
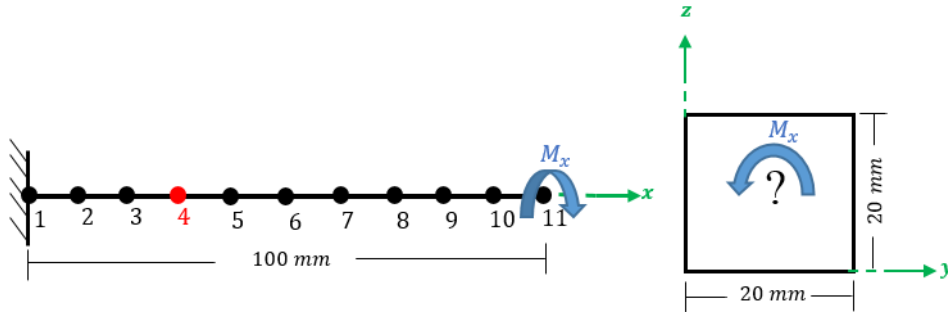
Figure 5.10. Force and Boundary Illustration of Problem 3

Like in the previous problem, the beam is modeled with 10 elements for resultants computation on the nodes. The 4th node, which is 30 mm far away from the fixed end, is selected as the location where optimization will be performed at. In each iteration, the calculated loads and moments on this node are used for stress evaluation and then for the optimization. Also, there is no symmetry constraint. The required data for the second optimization problem is tabulated below.

Table 5.7. *Specifications of Problem 3*

Load	Location of Load	Max. Stress Limit	Symmetry Constraint	Optimization Location
Twisting moment (M_x)	At the free end	250 MPa	(symy=0,symz=0)	$x = 30 \, mm$

Optimization Run 1

The first optimization run is done with the following setup parameters:

- Load values: $M_x = 100 \, N.m$

- Initial design: Four elements in the middle of the domain (Figure 5.11)

- Element addition and removal formula: $IR = 0.99 - 0.01 \, SS - 0.1 ON$ and $RC = 10$

- Meshing: 80x80 mesh (i.e. 6400 elements)

The optimization process stops to evolve at the 319th iteration where the maximum Von Mises stress value converges to the allowable one. After the iteration number 278, fine-tuning is proceeded by gradually removing elements from the domain .The obtained results depict a circular cross-section with a hole inside. This maximizes the polar moment of inertia which decreases the shear stress under the effects of uniform and non-uniform torque. These results are realistic and can be found in the literature [26]. The shear stresses increase as the distance from the center increases, as seen in Figure 5.11, which coincides with the classical beam theory.
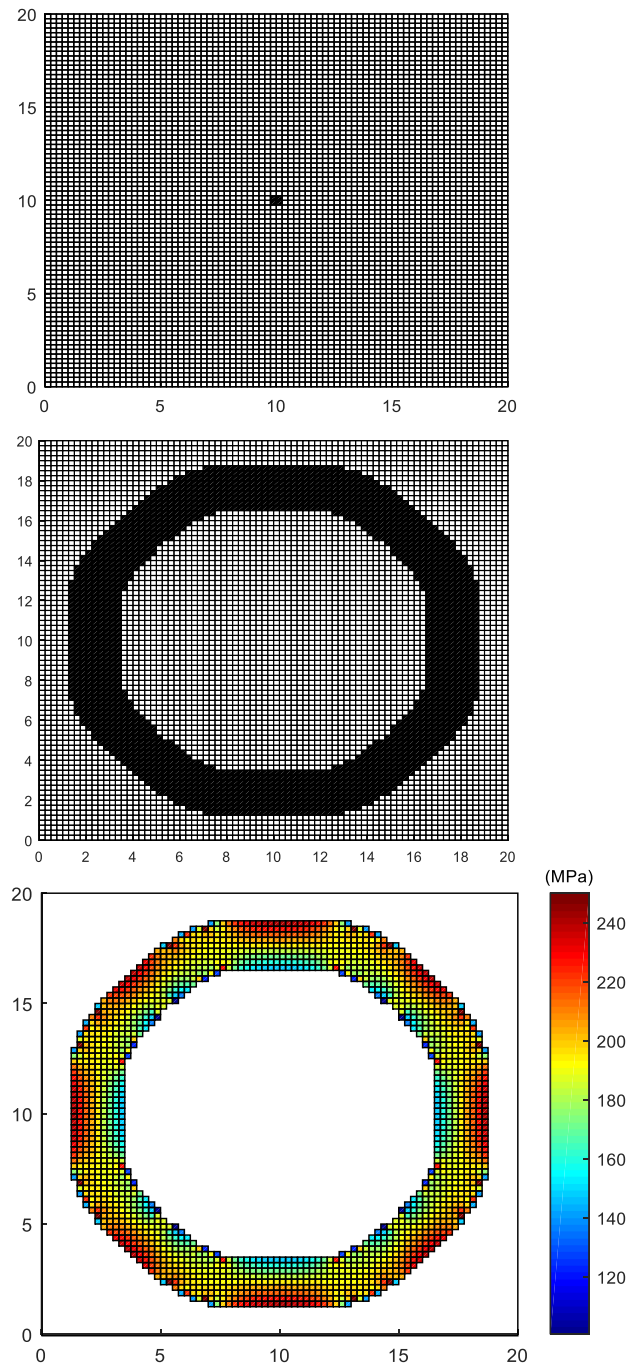
Figure 5.11. Optimization Run 1 for Problem 2: Initial Design Domain (Top), Optimized Cross-section (Middle), Von Mises Stress Distribution (Bottom)
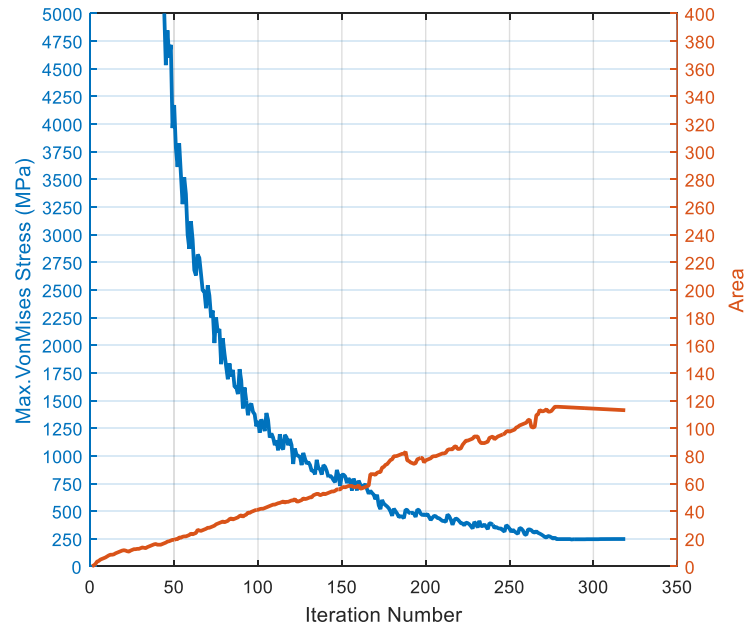
Figure 5.12. History of Maximum Stress and Area for the First Run of Optimization Run 1 for Problem 2

Optimization Run 2

The optimization methodology developed in this study (Evolutionary Growth Algorithm) provides the opportunity to start any initial design domain. Therefore, the optimization process is repeated with the new setup parameters in which the starting design and load value are changed.

- Load values: $M_x = 200\ N.m$

- Initial design: Thin walled square box (Figure 5.13)

- Element addition and removal formula: $IR = 0.99 - 0.01\ SS - 0.1ON$ and $RC = 10$

- Meshing: 80x80 mesh (i.e. 6400 elements)

The found cross-section for the changed setup parameters indicates a uniform hollow section with increased web plate thickness which is very similar to the one obtained in first run. This means that using a different starting domain and changing the value of the load does not affect the optimum topology significantly for this problem. This is because the beam is only subjected to a twisting moment and the St. Venant torque is the dominant resultant at the optimization point.
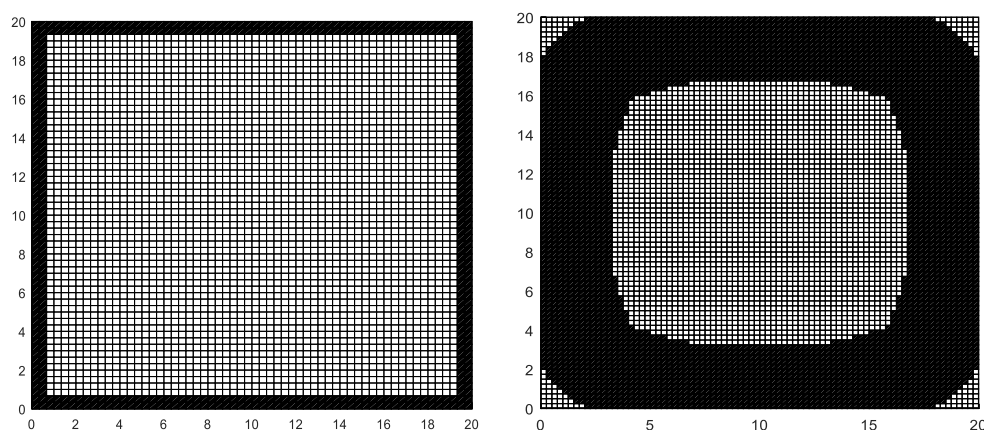
Figure 5.13. Optimization Run 2 for Problem 3: Initial Design Domain (Left), Optimized Cross Section (Right),

Also, when the results are compared to the solution of Kim and Kim [7] for the same boundary and force conditions, an analogous topology is proved. In their work, said authors investigate the maximization torsional constant at different mass constraints.
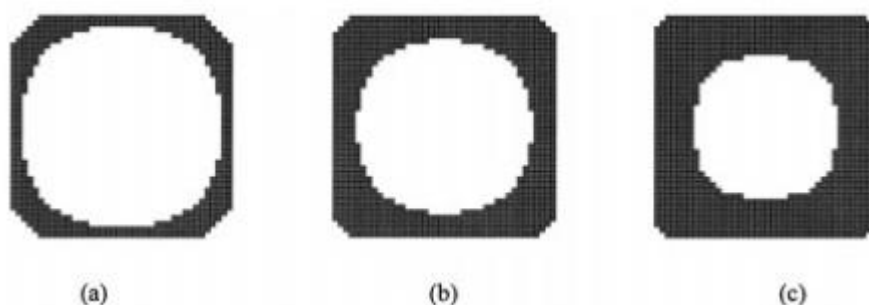
Figure 5.14. Result found by Kim and Kim [7] for Problem 3: (a)30% mass constraint,(b) 50% mass constraint, (c) 60% mass constraint

The summary of the results obtained for both optimization runs is given in the following tables.

Table 5.8. *Results Summary of Optimization Runs for Problem 3*

Run	Loading	Initial Design	Final Topology	Area	Max. Von Mises Stress
1	$M_x = 100.0 \, N.m$	Four elements in the middle	Circular hollow cross section	113 mm²	248.13 MPa
2	$M_x = 200.0 \, N.m$	Thin walled square box	Thick walled hollow square section	223.7 mm²	248.0 MPa

Table 5.9. *Geometric Properties of Found Cross Sections for Problem 3*

Run	Second Moments of Area			Torsional Constant	Warping Constant	Shear Center w.r.t centroid	
-	I_{yy} (mm^4)	I_{zz} (mm^4)	I_{yz} (mm^4)	J (mm^4)	I_w (mm^4)	Y_o (mm)	Z_o (mm)
1	3568	3568	0	6994	26.4	0	0
2	10375	10375	0	17829	6049	0	0

5.4. Case Study 4

The fourth problem is a case that combines Problem 1 and Problem 3. Both vertical load and a twisting moment are applied together at the free end of the beam.
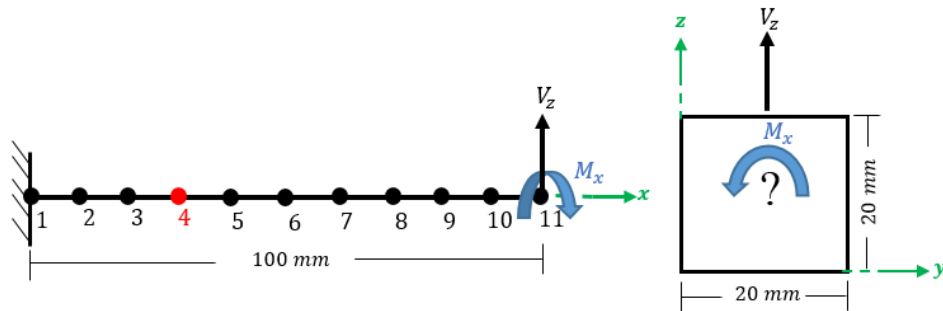
Figure 5.15. Force and Boundary Illustration of Problem 3

The same beam and maximum allowable cross-section domains are used for the topology optimization of this problem as in previous problems. The 4rd node, depicted in red in Figure 5.15, is selected as the optimization location for the section under no symmetry constraints..

Table 5.10. *Specifications of Problem 4*

Load	Location of Load	Max. Stress Limit	Symmetry Constraint	Optimization Location
Vertical Point Load (V_z) ——————— **Twisting moment** (M_x)	At the free end	250 MPa	(symy=0,symz=0)	$x = 30\ mm$

Optimization Run 1

The following setup parameters are used for the first optimization run.

- Load values: $V_z = 4.0 \ kN$ and $M_x = 50.0 \ N.m$
- Initial design: Four elements in the middle of the domain (Figure 5.18)
- Element addition and removal formula: $IR = 0.99 - 0.01 \ SS - 0.1ON$ and $RC = 10$
- Meshing: 60x60 mesh (i.e. 3600 elements)

At the optimization section of the beam (node number 4), while the bending moment is about y-axis, the vertical transverse loads are constant; uniform torque and non-uniform torque are changed throughout the process. Figure 5.16 represents the topologies in the intermediate iterations. In the earlier stages of the optimization, elements are introduced in the vertical direction and small holes are created. Up to iteration number 128, the topology of the section remains closed. After that iteration, the topology is converted into an open section. The maximum stress value oscillates greatly in the early stages of the optimization as seen from the evolution history (Figure 5.17). In subsequent iterations, the variation of the maximum stress value decreases and starts to converge towards the allowable stress limit. Finally, the "C'' type cross-section is attained after 300 iterations for the setup parameters specified for this run Although no symmetric condition is defined, the final topology is almost symmetric about the y-axis.
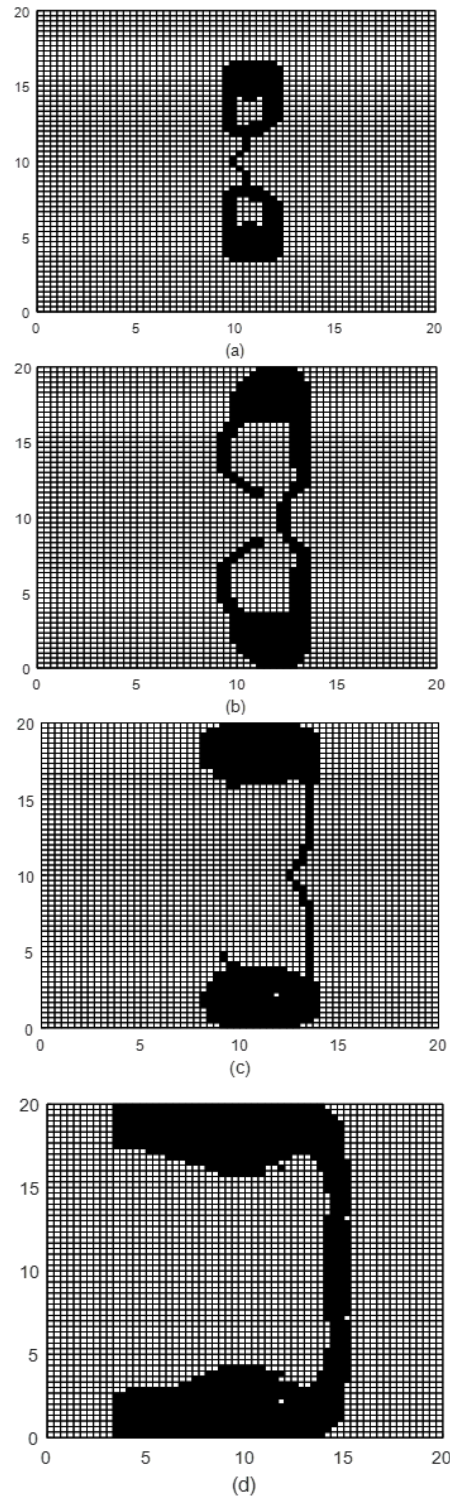
Figure 5.16. Intermediate Topologies of Optimization Run 1 for Problem 4, (a) Iteration=40,(b) Iteration=128,(c) Iteration=150,(d) Iteration=200
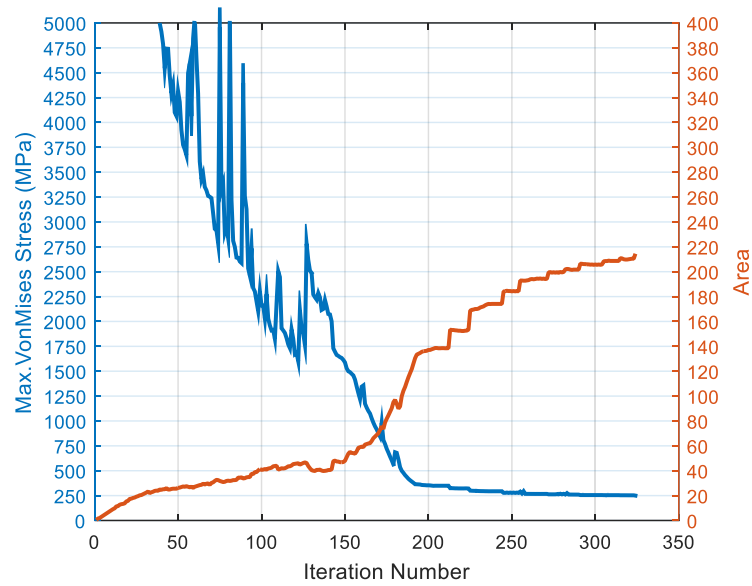
Figure 5.17. History of Maximum Stress and Area of the Optimization Run 1 for Problem 4

Shear stresses due to uniform torque and shear force are directed in the same direction at the right side of the structure. On the other hand, these are directed in the opposite direction on the left side of the section. Therefore, elements on the rights side have greater stress than those on the left side, which leads to the removal of elements from the left side and their addition to the right side. Besides shear stress, normal stresses owing to the bending moment are created on the upper and lower side of the domain. The stress distribution within the found section for the calculated resultants of the optimization node is seen in Figure 5.18.

Figure 5.18. Optimization Run 1 for Problem 4: Initial Design Domain (Top), Optimized Cross-section (Middle), Von Mises Stress Distribution (Bottom)

64

When the optimal topology is compared to that obtained by Liu et al. [2] a close resemblance is observed under similar loading and boundary conditions.

Figure 5.19. Result found by Liu et al. [2] for Problem

Optimization Run 2

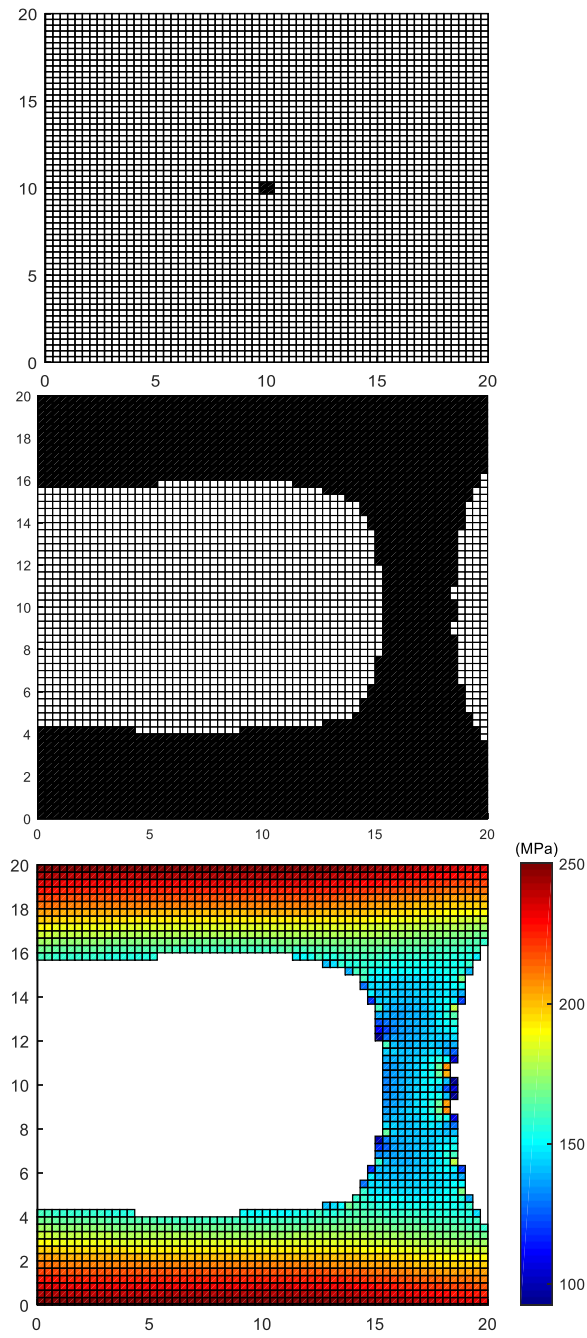In the second optimization run for Problem 4, only the values of the applied loads are changed in order to investigate the effect of the load magnitudes on the final topology while other setup parameters remain the same.

- Load values: $V_z = 2.0\ kN$ and $M_x = 100.0\ N.m$
- Initial design: Four elements in the middle of the domain (Figure 5.20)
- Element addition and removal formula: $IR = 0.99 - 0.01\ SS - 0.1ON$ and $RC = 10$
- Meshing: 60x60 mesh (i.e. 3600 elements)

This loading condition results in a nonsymmetrical closed box section in which one web is thicker than other(Figure 5.20). The results of the optimization for the previous loading are an open section. However, the Evolutionary Growth Algorithm ends up with a closed section for the changed loads. This shows that the final topology is highly dependent on the magnitude of the loads if the section is subjected to both transverse loading and torque.
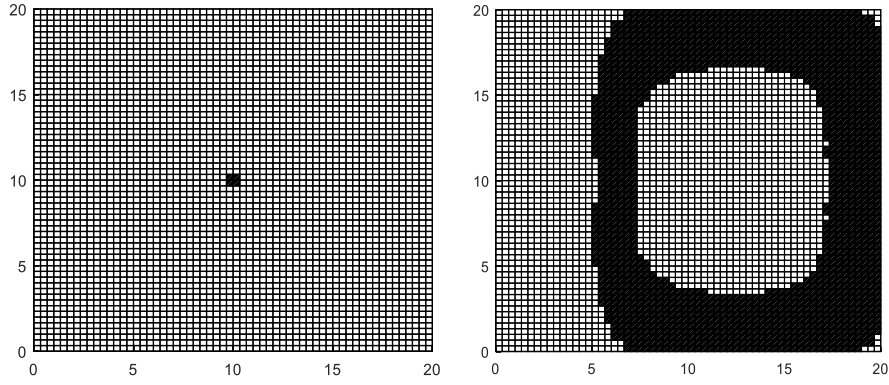
Figure 5.20. Optimization Run 2 for Problem 4: Initial Design Domain (Left), Optimized Cross Section (Right)

The geometric properties of the obtained cross sections and the Von Mises stress values are summarized in the following tables.

Table 5.11. *Results Summary of the Optimization Runs for Problem 4*

Run	Loading	Initial Design	Final Topology	Area	Max. Von Mises Stress
1	$V_z = 4.0\ kN$ $M_x = 50.0\ N.m$	4 elements in the middle	"C" type cross section	214.4 mm^2	249.83 MPa
2	$V_z = 2.0\ kN$ $M_x = 100.0\ N.m$	4 elements in the middle	Non-symmetric rectangular hollow	172.4 mm^2	249.86 MPa

Table 5.12. *Geometric Properties of the Found Cross-sections for Problem 4*

Run	Moment of Inertia			Torsional Constant	Warping Constant	Shear Center w.r.t centroid	
-	I_{yy} (mm^4)	I_{zz} (mm^4)	I_{yz} (mm^4)	J (mm^4)	I_w (mm^4)	Y_o (mm)	Z_o (mm)
1	11349	7385	4.2	1340	402603	11.1	0
2	7897	4276	0	9439	19564	0.33	0

66

5.5. Case Study 5

In the last problem, a vertical transverse load, an axial load and a twist moment are applied at the free end of beam simultaneously. The beam length and beam properties are the same as the previous examples. Moreover, the optimization location on the beam has not been altered.
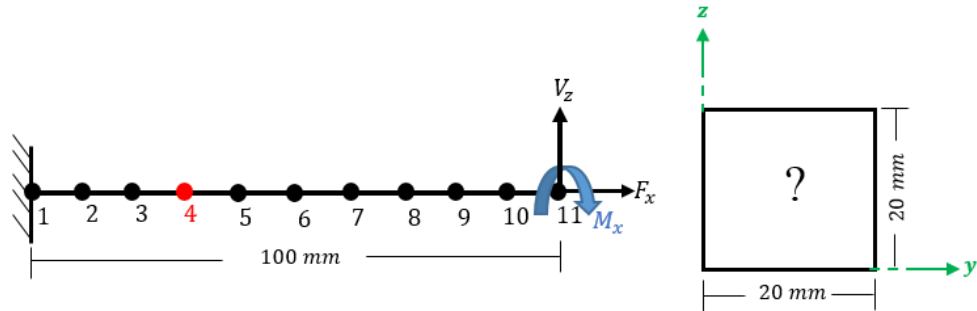
Figure 5.21. Force and Boundary Illustration of Problem 5

As it can be seen in the table below, which summarizes Problem 5, symmetry about the z-axis is desired at the end of the process.

Table 5.13. *Specifications of Problem 5*

Load	Location of Load	Max. Stress Limit	Symmetry Constraint	Optimization Location
Vertical Point Load (V_z)				
Twisting moment (M_x)	At the free end	250 MPa	(symy=0,symz=1)	$x = 30 \ mm$
Axial Load(F_x)				

Optimization Run 1

The following setup parameters are used for the first optimization run.

- Load values: $F_x = 10.0\ kN, V_z = 1.0\ kN$ and $M_x = 50.0\ N.m$
- Initial design: two rows elements from middle to left boundary and bottom boundary (Figure 5.24)
- Element addition and removal formula: $IR = 0.96 - 0.01\ SS - 0.1ON$ and $RC = 15$
- Meshing: 60x60 mesh (i.e. 3600 elements)

Optimization can be commenced with these chosen parameters. At the beginning elements lying to the left side of the domain are removed from the structure, because these elements have the lowest stress levels and the elements can be added to the middle of the domain. Then, in subsequent iterations, the section grows radially in the middle, and horizontally at the bottom. During the evolution, an elliptic hole, symmetric about the z-axis, is created as indicated in Figure 5.22, which shows the intermediate steps of the optimization Run 1.
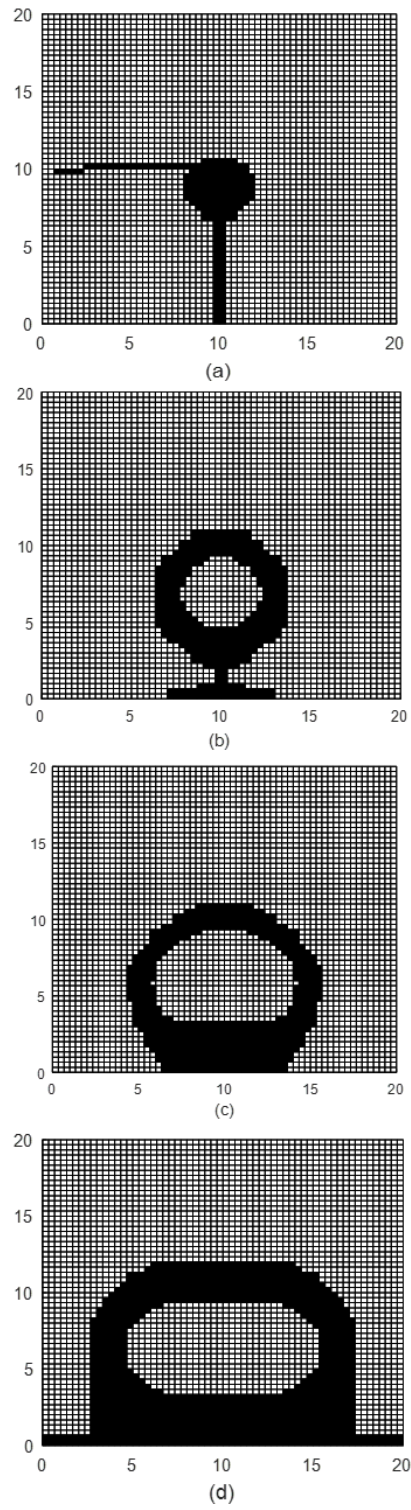
Figure 5.22. Intermediate Topologies of the Optimization Run 1 for Problem 5

69

Shear stresses due to twisting moment and shear force are directed in the same direction at the right side of the structure. Moreover, normal stress is higher on the bottom of the section because both the bending moment and normal force create tensile normal stresses in the elements under the centroid. Therefore, a , nonsymmetrical hollow section in which the bottom side is thicker than the upper side is created. On the other hand, it is expected that the right side is thicker than the left side due to the direction of shear stresses, as in the case of the previous problem. Nevertheless, the presence of symmetric design constraint about the z-axis causes the right and left side to be the same thickness. Figure 5.24 displays initial design domain, optimized cross section topology and the Von Mises stress distribution within the final cross-section at the optimization node.

Although the optimization process begins with non-symmetric structure, at the end symmetric cross-section about z, as desired, is resulted. Optimized cross-section of the beam under the defined loads and design constraints is found at the 248th iteration. Only the last ten iterations belong fine-tuning part.

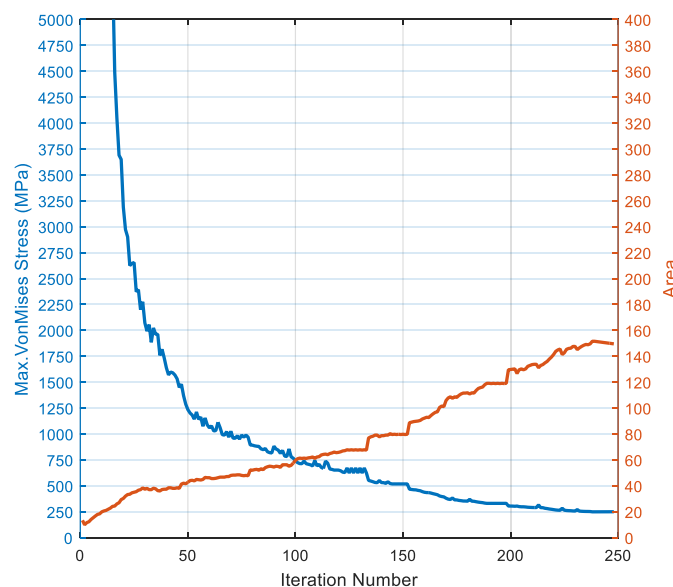

Figure 5.23. History of Maximum Stress and Area of the Optimization Run 1 for Problem 5
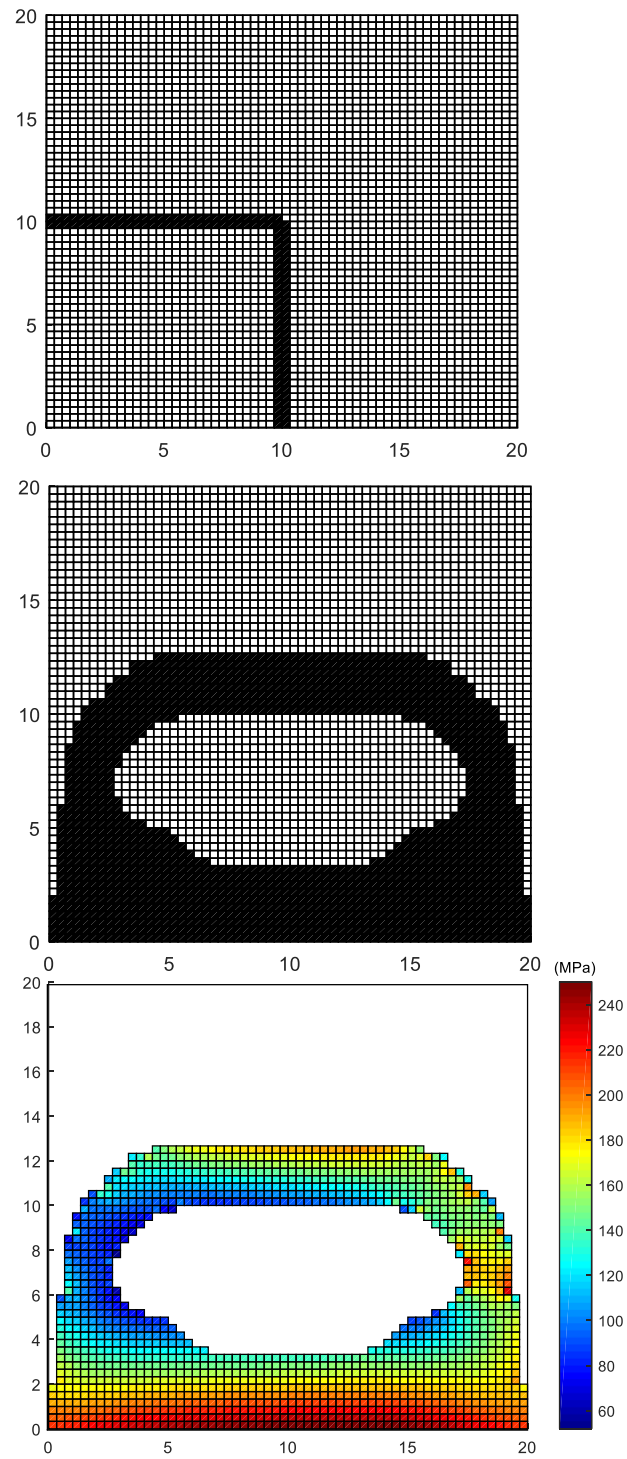
Figure 5.24. Optimization Run 1 for Problem 5: Initial Design Domain (Top), Optimized Cross-section (Middle), Von Mises Stress Distribution (Bottom)

71

Optimization Run 2

As a second run, this problem is solved for a different initial design domain while the other setup parameters remain the same

- Load values: $F_x = 10.0\ kN, V_z = 1.0\ kN$ and $M_x = 50.0\ N.m$
- Initial design: four elements in the middle of the domain(Figure 5.25)
- Element addition and removal formula: $IR = 0.96 - 0.01\ SS - 0.1ON$ and $RC = 15$
- Meshing: 60x60 mesh (i.e. 3600 elements)

When the optimization process starts to evolve from the initial domain (with four elements in the middle) the obtained result looks like the one obtained in the first optimization run as shown in the figure below.
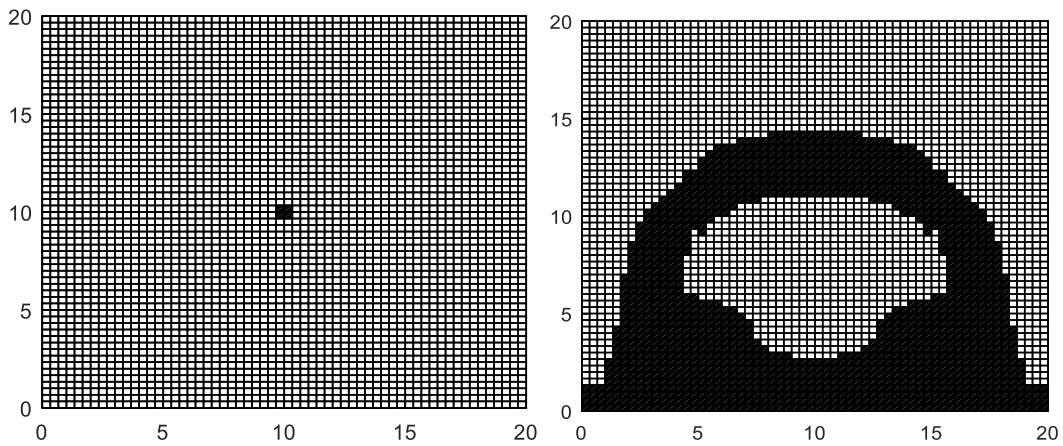

Figure 5.25. Optimization Run 2 for Problem 5: Initial Design Domain (Left), Optimized Cross-section (Right),

The numerical results of the optimization runs performed for this problem are summarized in Table 5.14 and Table 5.15

Table 5.14. *Results Summary of the Optimization Runs for Problem 5*

Run	Loading	Initial Design	Final Topology	Area	Max. Von Mises Stress
1	$V_z = 1.0\ kN$ $M_x = 50.0\ N.m$ $F_x = 10.0\ kN$	See Figure 5.24	See Figure 5.24	149.56 mm^2	249.3 MPa
2	$V_z = 1.0\ kN$ $M_x = 50.0\ N.m$ $F_x = 10.0\ kN$	See Figure 5.25	See Figure 5.25	148.89 mm^2	249.7 MPa

Table 5.15. *Geometric Properties of the Found Cross Sections for Problem 5*

Run	Moment of Inertia			Torsional Constant	Warping Constant	Shear Center w.r.t centroid	
-	I_{yy} (mm^4)	I_{zz} (mm^4)	I_{yz} (mm^4)	J (mm^4)	I_w (mm^4)	Y_o (mm)	Z_o (mm)
1	2566	5458	0	5869	5850	0	0.15
2	2934	4258	0	5487	2793	0	0.38

CHAPTER 6

CONCLUSION AND FUTURE WORKS

6.1. Summary

The optimum topology of the Vlasov beam cross-sections under different loading conditions are investigated by the novel method proposed in this thesis. Although the main focus is the optimization procedure, a detailed explanation on the finite element method for determination of force resultants and stresses over cross-sections is given in the formulation chapter. The idea behind the proposed method and the optimization process is also mentioned in the optimization formulation section. Even though the optimization technique employed in this study resembles the classical BESO method, it is different in many respects. In the literature, most of the BESO applications are based on mean compliance minimization with a volume constraint. The convergence criteria of BESO are determined by predefined volume fractions. However, these are not physical limitations of the structure and so their use results in significantly different topology for different volume constraints. For this reason, the stress limitation for the defined cross-section is introduced in the optimization algorithm as a convergence criterion. While the BESO approach is required to start with a full domain and the element properties for all elements are changed during the optimization process, the proposed technique in this study can start with any domain; and, it is sufficient to change only the status of the elements to be removed and added. Cross-section optimization is initiated from an estimated initial design starting point, from which it continues to evolve, until the maximum stress limit of the section converges to the prescribed limit.

The symmetry design constraint is designated for some problems to determine the efficiency of the optimization method. In addition, as it can be seen in the results of

case studies, all of the optimized sections maintain structural integrity through inverted subroutine controlling the connectivity of the elements.

Element addition decreases the maximum stress and element removal enhances its value. Elements are added to the domain in such a manner that the number of added or reintroduced elements is controlled by the inclusion rate, which restricts the number of elements to be included in one iteration. In order to fully distribute the stresses within the design, the maximum stress of the section must be as close as possible to the stress limit. Therefore, a fine-tuning algorithm, which is another improvement made in the proposed method, is embedded into the optimization algorithm as mentioned in Chapter 4.

Five numerical examples have been solved in order to validate the proposed method− the Evolutionary Growth Algorithm. In the first and second case studies, the optimization algorithm was run only once for the specified setup parameters and the obtained results are summarized within this body of work. On the other hand, in other problems, two optimization runs were performed with different setup parameters in order to investigate the effects of initial design domain and magnitude of the applied loads on the cross-section topology.

6.2. Conclusion

In the case studies, a tip loaded cantilevered beam is analyzed for different loading conditions. From the results of case studies, inferences can be summarized as follows:

- The results of Problem 1 and Problem 5 show that the proposed method works properly to generate the topology satisfying symmetry design constraint.
- In all examples, the maximum stress converges to the limit within the desired error rate.
- The beam under only vertical loading results in an "I" type cross-section structure when symmetry about the z-axis is introduced. In addition to this, the

optimized section is fitted with minimum weight in a maximum design domain.

- When only a twisting moment is applied at the end of the beam and 4 elements in the middle of the domain are selected as the initial design, a circular hollow cross-section is obtained in the presence of the symmetry constraint.

- A "C" type cross section structure is obtained when both a vertical load and twisting moment are applied. If the twisting moment is increased, a nonsymmetrical rectangular box type cross-section is created as the optimum solution.

- In general, it is noted from the numerical examples that if the local minimum stress points are distinct, then the final design is dependent on the initial design. Otherwise, the final design may not be dependent on the initial design, as in Problem 3 and Problem 5. Elements under relevantly lower stress are very close to each other in all iterations. Therefore, using a different initial design does not change the final topology.

6.3. Future Works

The lateral torsional buckling constraint has not been considered in the present study. This can be included in a future work. Furthermore, a variable cross section design considering the entire beam can be carried out by using a 3D design domain consisting of cubic finite elements.

REFERENCES

[1] Oğuz Ziya Tikenoğulları, "Bi-Directional Evolutionary Algorithm for Volume Constrained Topology Optimization Of Axisymmetric Solids," 2015.

[2] M. Abdi, I. Ashcroft, and R. Wildman, "An X-FEM based approach for topology optimization of continuum structures," in *Advances in Intelligent Systems and Computing*, 2014.

[3] E. Biyikli and A. C. To, "Proportional topology optimization: A new non-sensitivity method for solving stress constrained and minimum compliance problems and its implementation in MATLAB," *PLoS One*, 2015.

[4] Y. M. Xie and G. P. Steven, "A simple evolutionary procedure for structural optimization," *Comput. Struct.*, 1993.

[5] O. M. Querin, V. Young, G. P. Steven, and Y. M. Xie, "Computational efficiency and validation of bi-directional evolutionary structural optimization," *Comput. Methods Appl. Mech. Eng.*, 2000.

[6] R. H. Zuberi, Z. Zhengxing, and L. Kai, "Topological optimization of beam cross section by employing extrusion constraint," in *AIP Conference Proceedings*, 2010.

[7] Y. Y. Kim and T. S. Kim, "Topology optimization of beam cross sections," *Int. J. Solids Struct.*, 2000.

[8] M. P. Bendsøe and N. Kikuchi, "Generating optimal topologies in structural design using a homogenization method," *Comput. Methods Appl. Mech. Eng.*, 1988.

[9] J. Guedes and N. Kikuchi, "Preprocessing and postprocessing for materials based on the homogenization method with adaptive finite element methods," *Comput. Methods Appl. Mech. Eng.*, 1990.

[10] K. Suzuki and N. Kikuchi, "A homogenization method for shape and topology optimization," *Comput. Methods Appl. Mech. Eng.*, 1991.

[11] N. Olhoff, M. P. Bendsøe, and J. Rasmussen, "On CAD-integrated structural topology and design optimization," *Comput. Methods Appl. Mech. Eng.*, 1991.

[12] C. S. Jog, R. B. Haber, and M. P. Bendsøe, "Topology design with optimized, self-adaptive materials," *Int. J. Numer. Methods Eng.*, 1994.

[13] S. Liu, X. An, and H. Jia, "Topology optimization of beam cross-section considering warping deformation," *Struct. Multidiscip. Optim.*, vol. 35, no. 5, pp. 403–411, May 2008.

[14]   M. I. Frecker, G. K. Ananthasuresh, S. Nishiwaki, N. Kikuchi, and S. Kota, "Topological Synthesis of Compliant Mechanisms Using Multi-Criteria Optimization," *J. Mech. Des.*, 1997.

[15]   A. Rietz, "Sufficiency of a finite exponent in SIMP (power law) methods," *Struct. Multidiscip. Optim.*, 2001.

[16]   M. P. Bendsøe, "Optimal shape design as a material distribution problem," *Struct. Optim.*, 1989.

[17]   N. Andelić, V. M. Mitić, and T. Maneski, "An approach to the optimization of a thin-walled Z-beam," *Stroj. Vestnik/Journal Mech. Eng.*, 2009.

[18]   D. R. Griffiths and J. C. Miles, "Determining the optimal cross-section of beams," *Adv. Eng. Informatics*, 2003.

[19]   K. Proos and B. E. Hons, "Evolutionary Structural Optimisation as a Robust and Reliable Design Tool," *Analysis*, 2002.

[20]   Semih ERDOĞAN, "DETERMINATION OF STRESSES IN VLASOV BEAMS," MIDDLE EAST TECHNICAL UNIVERSITY, 2019.

[21]   J. Fish and T. Belytschko, *A First Course in Finite Elements*. 2007.

[22]   W. D. Pilkey, "Beam Elements," in *Analysis and Design of Elastic Beams*, 2007.

[23]   O. Sigmund, "On the design of compliant mechanisms using topology optimization," *Mech. Struct. Mach.*, 1997.

[24]   D. J. Munk, G. A. Vio, and G. P. Steven, "A Bi-directional Evolutionary Structural Optimisation algorithm with an added connectivity constraint," *Finite Elem. Anal. Des.*, vol. 131, no. April, pp. 25–42, 2017.

[25]   K. ISHII and S. AOMURA, "Topology Optimization for the Extruded Three Dimensional Structure with Constant Cross Section.," *Trans. Japan Soc. Mech. Eng. Ser. A*, 2011.

[26]   V. T. Troshchenko and R. I. Kuriat, "Strength of materials and structures," in *Strength of Materials*, 2006.